CDF-QCD Data for Theorists
Part 1 "Leading Jet Events"

Rick Field
Department of Physics, University of Florida
Gainesville, Florida, 32611, USA

and

Craig Group
Fermilab, P.O. Box 500
Batavia, IL 60510-5011, USA

November 1, 2007

Abstract

We study the behavior of charged particles ($p_T > 0.5$ GeV/c, $|\eta| < 1$) and energy ($|\eta| < 1$) produced in association with large transverse momentum jets in proton-antiproton collisions at 1.96 TeV. We use the direction of the leading jet in each event to define three regions of η-ϕ space; "toward", "away", and "transverse". The "transverse" region is very sensitive to the "underlying event" and is separated into a MAX and MIN "transverse" region, which helps separate the "hard component" (initial and final-state radiation) from the "beam-beam remnant" and multiple parton interaction components of the scattering. In addition, we study four distinct jet topologies. We refer to events in which the only restriction is that the leading jet lie in the region $|\eta| < 2$ as "leading jet" events. "Back-to-back inclusive 2-jet" events are a subset of the "leading jet" events which have at least two jets that are nearly back-to-back ($\Delta\phi_{12} > 150^o$) and $E_T(\text{jet\#2})/E_T(\text{jet\#1}) > 0.8$. "Back-to-back exclusive 2-jet" events are a subset of the "back-to-back inclusive 2-jet" events which in addition have $p_T(\text{jet\#3}) < 15$ GeV/c. For "leading chgjet" events we look only at charged particles ($p_T > 0.5$, $|\eta| < 1$) and construct charged particle jets. The data are corrected to the particle level and are then compared with the PYTHIA Tune A (with multiple parton interactions) and HERWIG (without multiple parton interactions) at the particle level (*i.e.* generator level). The goal is to produce data that can be used by the theorists to tune and improve the QCD Monte-Carlo models that are used to simulate hadron-hadron collisions. In this note we show the results of the "leading jet" topology. The other three topologies will be presented in subsequent notes.

I. Introduction

The goal of this analysis is to produce data that can be used by the theorists to tune and improve the QCD Monte-Carlo models. Fig. 1 illustrates the way the QCD Monte-Carlo models simulate a proton-antiproton collision in which a "hard" 2-to-2 parton scattering with transverse momentum, p_T(hard), has occurred. The resulting event contains particles that originate from the two outgoing partons (*plus initial and final-state radiation*) and particles that come from the breakup of the proton and antiproton (*i.e.* "beam-beam remnants"). The "underlying event" is everything except the two outgoing hard scattered "jets" and receives contributions from the "beam-beam remnants" plus initial and final-state radiation. The "hard scattering" component consists of the outgoing two jets plus initial and final-state radiation.

The "beam-beam remnants" are what is left over after a parton is knocked out of each of the initial two beam hadrons. It is the reason hadron-hadron collisions are more "messy" than electron-positron annihilations and no one really knows how it should be modeled. For the QCD Monte-Carlo models the "beam-beam remnants" are an important component of the "underlying event". Also, it is possible that multiple parton scattering contributes to the "underlying event". Fig. 2 shows the way PYTHIA [1] models the "underlying event" in proton-antiproton collision by including multiple parton interactions. In addition to the hard 2-to-2 parton-parton scattering and the "beam-beam remnants", sometimes there is a second "semi-hard" 2-to-2 parton-parton scattering that contributes particles to the "underlying event".

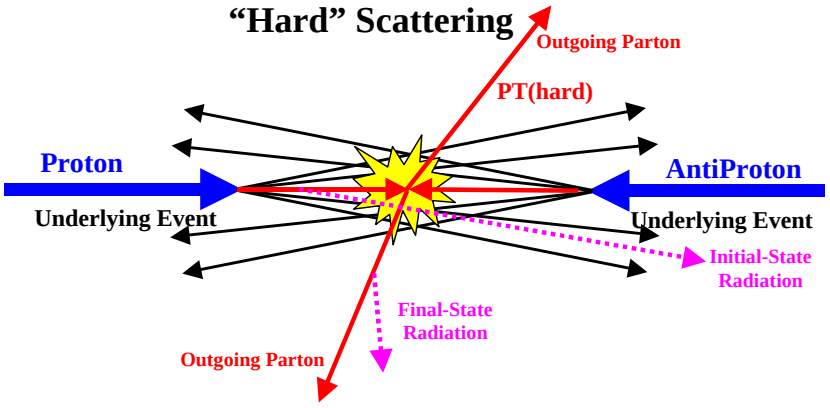

Fig. 1. Illustration of the way QCD Monte-Carlo models simulate a proton-antiproton collision in which a "hard" 2-to-2 parton scattering with transverse momentum, P_T(hard), has occurred. The resulting event contains particles that originate from the two outgoing partons (plus initial and final-state radiation) and particles that come from the breakup of the proton and antiproton (*i.e.* "beam-beam remnants"). The "underlying event" is everything except the two outgoing hard scattered "jets" and consists of the "beam-beam remnants" plus initial and final-state radiation. The "hard scattering" component consists of the outgoing two jets plus initial and final-state radiation.

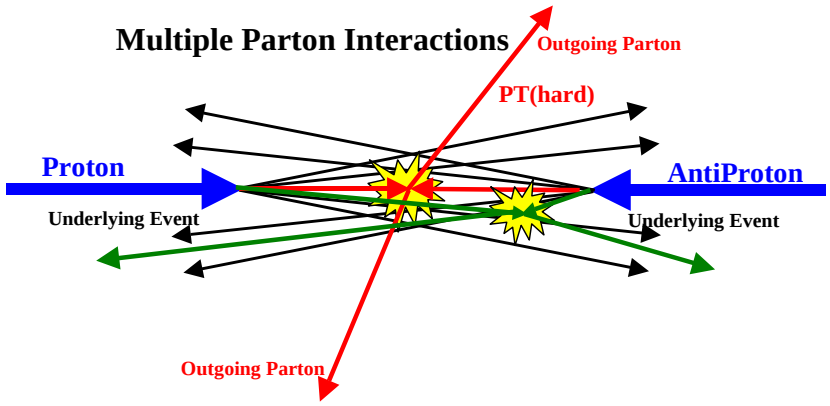

Fig. 2. Illustration of the way PYTHIA models the "underlying event" in proton-antiproton collision by including multiple parton interactions. In addition to the hard 2-to-2 parton-parton scattering with transverse momentum, P_T(hard), there is a second "semi-hard" 2-to-2 parton-parton scattering that contributes particles to the "underlying event".

Hard scattering collider "jet" events have a distinct topology. On the average, the outgoing hadrons "remember" the underlying the 2-to-2 hard scattering subprocess. An typical hard scattering event consists of a collection (or burst) of hadrons traveling roughly in the direction of the initial two beam particles and two collections of hadrons (*i.e.* "jets") with large transverse momentum. The two large transverse momentum "jets" are roughly back to back in azimuthal angle. One can use the topological structure of hadron-hadron collisions to study the

"underlying event" [2-4]. We use the direction of the leading jet in each event to define three regions of η-ϕ space.

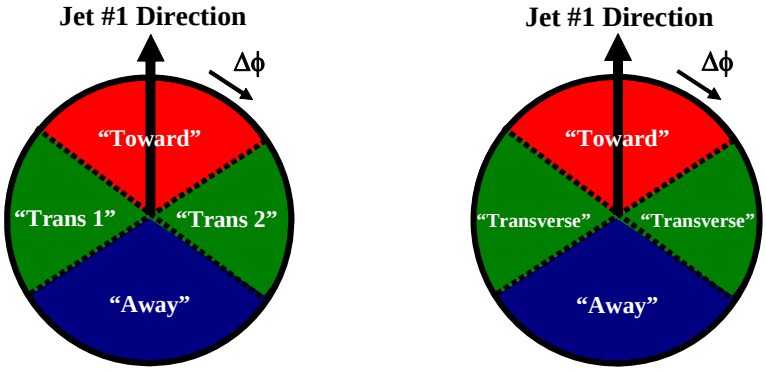

Fig. 3. (*left*) Illustration of correlations in azimuthal angle Δϕ relative to the direction of the leading jet (highest P_T jet) in the event, jet#1. The angle $\Delta\phi = \phi - \phi_{jet\#1}$ is the relative azimuthal angle between charged particles and the direction of jet#1. The "toward" region is defined by $|\Delta\phi| < 60^o$ and $|\eta| < 1$, while the "away" region is $|\Delta\phi| > 120^o$ and $|\eta| < 1$. The two "transverse" regions $60^o < \Delta\phi < 120^o$ and $60^o < -\Delta\phi < 120^o$ are referred to as "transverse 1" and "transverse 2". Each of the two "transverse" regions have an area in η-ϕ space of $\Delta\eta\Delta\phi = 4\pi/6$. The overall "transverse" region (*right*) corresponds to combining the "transverse 1" and "transverse 2" regions.

As illustrated in Fig. 3, the direction of the leading jet, jet#1, is used to define correlations in the azimuthal angle, Δϕ. The angle $\Delta\phi = \phi - \phi_{jet\#1}$ is the relative azimuthal angle between a charged particle (or a calorimeter tower) and the direction of jet#1. The "toward" and "away" regions are sensitive to the outgoing high p_T jets, while the "transverse" region is perpendicular to the plane of the hard 2-to-2 scattering and is therefore very sensitive to the "underlying event". We study charged particles in the range $p_T > 0.5$ GeV/c and $|\eta| < 1$ and calorimeter towers with $E_T > 0.1$ GeV and $|\eta| < 1$ in the "toward", "away" and "transverse" regions. However as shown in Fig. 4, we allow the leading calorimeter jet that defines the three regions to be in the region $|\eta| < 2$.

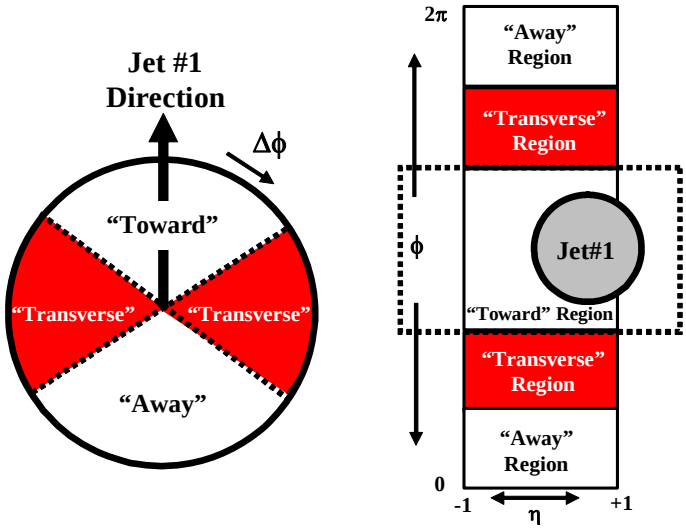

Fig. 4. Illustration of correlations in azimuthal angle Δϕ relative to the direction of the leading jet (MidPoint, R = 0.7, f_{merge} = 0.75) in the event, jet#1. The angle $\Delta\phi = \phi - \phi_{jet\#1}$ is the relative azimuthal angle between charged particles (or calorimeter towers) and the direction of jet#1. The "toward" region is defined by $|\Delta\phi| < 60^o$ and $|\eta| < 1$, while the "away" region is $|\Delta\phi| > 120^o$ and $|\eta| < 1$. The "transverse" region is defined by $60^o < |\Delta\phi| < 120^o$ and $|\eta| < 1$. Each of the three regions "toward", "transverse", and "away" and has an overall area in η-ϕ space of $\Delta\eta\Delta\phi = 4\pi/3$. We examine charged particles in the range $p_T >$

0.5 GeV/c and $|\eta| < 1$ and calorimeter towers with $E_T > 0.1$ GeV and $|\eta| < 1$, but allow the leading jet to be in the region $|\eta(\text{jet\#1})| < 2$.

The overall "transverse" region corresponds to combining the "transverse 1" and "transverse 2" regions shown in Fig. 3. As shown in Fig. 5, we define a variety of MAX and MIN "transverse" regions ("transMAX" and "transMIN") which helps separate the "hard component" (initial and final-state radiation) from the "beam-beam remnant" component (see Fig. 6). MAX (MIN) refer to the "transverse" region containing largest (smallest) number of charged particles or to the region containing the largest (smallest) scalar p_T sum of charged particles or the region containing the largest (smallest) scalar E_T sum of particles.

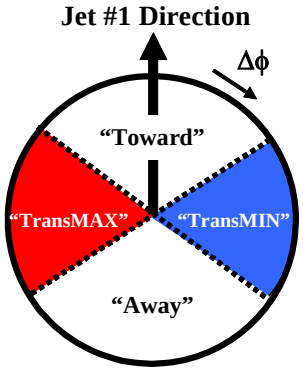

Fig. 5. Illustration of correlations in azimuthal angle $\Delta\phi$ relative to the direction of the leading jet (highest P_T jet) in the event, jet#1 for "leading jet" events (*left*) and "back-to-back" events (*right*) as defined in Fig. 4. The angle $\Delta\phi = \phi - \phi_{\text{jet\#1}}$ is the relative azimuthal angle between charged particles (or calorimeter towers) and the direction of jet#1. On an event by event basis, we define "transMAX" ("transMIN") to be the maximum (minimum) of the two "transverse" regions, $60^o < \Delta\phi < 120^o$ and $60^o < -\Delta\phi < 120^o$. "TransMAX" and "transMIN" each have an area in η-ϕ space of $\Delta\eta\Delta\phi = 4\pi/6$. The overall "transverse" region defined in Fig. 4 includes both the "transMAX" and the "transMIN" region.

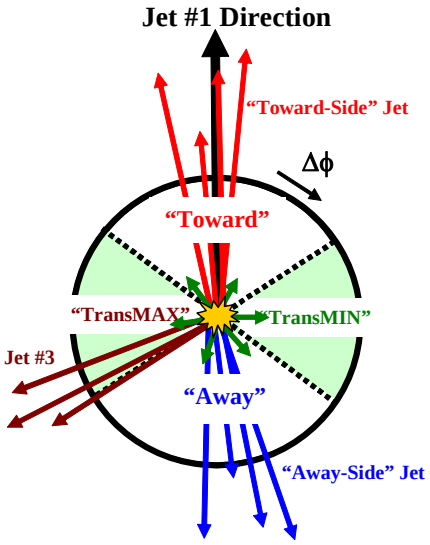

Fig. 6. Illustration of the topology of a proton-antiproton collision in which a "hard" parton-parton collision has occurred. The "toward" region as defined in Fig. 3 contains the leading "jet", while the "away" region, on the average, contains the "away-side" "jet". The "transverse" region is perpendicular to the plane of the hard 2-to-2 scattering and is very sensitive to the "underlying event". For events with large initial or final-state radiation the "transMAX" region defined in Fig.5 would contain the third jet while both the "transMAX" and "transMIN" regions receive contributions from the beam-beam remnants (see Fig.

1). Thus, the "transMIN" region is very sensitive to the beam-beam remnants, while the "transMAX" minus the "transMIN" (*i.e.* "transDIF") is very sensitive to initial and final-state radiation.

In addition, as shown in Table 1 we study four distinct jet topologies. We refer to events in which the only restriction is that the leading jet lie in the region $|\eta| < 2$ as "leading jet" events. "Back-to-back inclusive 2-jet" events are a subset of the "leading jet" events which have at least two jets that are nearly back-to-back ($\Delta\phi_{12} > 150^o$) and $E_T(\text{jet\#2})/E_T(\text{jet\#1}) > 0.8$. "Back-to-back exclusive 2-jet" events are a subset of the "back-to-back inclusive 2-jet" events which in addition have $P_T(\text{jet\#3}) < 15$ GeV/c. For "leading chgjet" events we look only at charged particles ($p_T > 0.5$, $|\eta| < 1$) and construct charged particle jets.

The two "back-to-back" topologies suppress hard initial and final-state radiation thus increasing the sensitivity of the "transverse" region to the "beam-beam remnant" and the multiple parton scattering component of the "underlying event". By comparing the inclusive and exclusive back-to-back 2-jet topologies one learns about the importance of contributions from third jet. The "leading chgjet" study is similar to the Run 1 "underlying event" analysis [2] since it does not involve calorimeter jets and it is instructive to compare the "leading jet" and "leading chgjet" results.

Table 1. Definition of the four jet topologies used in this analysis.

Name	Selection Criterion
"Leading Jet"	Require the leading jet, jet#1, to have $\|\eta(\text{jet\#1})\| < 2$.
"Back-to-Back Inc2J"	Require at least two jets with $\|\eta(\text{jet})\| < 2$. In addition require $\|\Delta\phi_{12}\| > 150^o$ and $P_T(\text{jet\#2})/P_T(\text{jet\#1}) > 0.8$.
"Back-to-Back Exc2J"	Require at least two jets with $\|\eta(\text{jet})\| < 2$. In addition require $\|\Delta\phi_{12}\| > 150^o$, $P_T(\text{jet\#2})/P_T(\text{jet\#1}) > 0.8$, and $P_T(\text{jet\#3}) < 15$ GeV/c.
"Leading ChgJet"	Look only at charged particles ($p_T > 0.5$, $\|\eta\| < 1$) and construct charged particle jets.

Table 2 shows some of the observables that are considered in this analysis as they are defined at the particle level and detector level. Since we will be studying regions in η-ϕ space with different areas, we will construct densities by dividing by the area. For example, the number density, $dN/d\eta d\phi$, corresponds the number of charged particles per unit η-ϕ and the PTsum density, $dPT/d\eta d\phi$, corresponds the amount of charged scalar p_T sum per unit η-ϕ, and the ETsum density, $dET/d\eta d\phi$, corresponds the amount of scalar E_T sum per unit η-ϕ.

The calorimeter jets are constructed using the MidPoint algorithm ($R = 0.7$, $f_{merge} = 0.75$) and the charged particle jets are constructed using the simple algorithm we used in the Run 1 analysis [2]. The data are corrected to the particle level. The corrected observables are then compared with PYTHIA Tune A (with multiple parton interactions) [5] and HERWIG (without multiple parton interactions) [6] at the particle level (*i.e.* generator level).

In Section II we discuss the data selection and the track cuts. The method we use to correct the data to the particle level is presented in Section III and the resulting data for "leading jet" events are shown in Section IV. The other three topologies will be presented in subsequent notes. Section V is reserved for the summary and conclusions.

Table 2. Observables examined in this analysis as they are defined at the particle level and the detector level. Charged tracks are considered "good" if they pass the selection criterion given in Table 5. The mean charged particle $<p_T>$ and the charged fraction PTsum/ETsum are constructed on and event-by-event basis and then averaged over the events. For the average p_T and the PTmax we require that there is at least one charge particle present. The PTsum density is taken to be zero if there are no charged particles present.

Observable	Particle Level	Detector level
$dN/d\eta d\phi$	Number of charged particles per unit η-ϕ ($p_T > 0.5$ GeV/c, $\|\eta\| < 1$)	Number of "good" charged tracks per unit η-ϕ ($p_T > 0.5$ GeV/c, $\|\eta\| < 1$)
$dPT/d\eta d\phi$	Scalar p_T sum of charged particles per unit η-ϕ ($p_T > 0.5$ GeV/c, $\|\eta\| < 1$)	Scalar p_T sum of "good" charged tracks per unit η-ϕ ($p_T > 0.5$ GeV/c, $\|\eta\| < 1$)
$<p_T>$	Average p_T of charged particles ($p_T > 0.5$ GeV/c, $\|\eta\| < 1$) Require at least 1 charged particle	Average p_T of "good" charged tracks ($p_T > 0.5$ GeV/c, $\|\eta\| < 1$) Require at least 1 "good" track
PTmax	Maximum p_T charged particle ($p_T > 0.5$ GeV/c, $\|\eta\| < 1$) Require at least 1 charged particle	Maximum p_T "good" charged tracks ($p_T > 0.5$ GeV/c, $\|\eta\| < 1$) Require at least 1 "good" track
$dET/d\eta d\phi$	Scalar E_T sum of all particles per unit η-ϕ (all p_T, $\|\eta\| < 1$)	Scalar E_T sum of all calorimeter towers per unit η-ϕ ($E_T > 0.1$ GeV, $\|\eta\| < 1$)
ChgFr= PTsum/ETsum	Scalar p_T sum of charged particles ($p_T > 0.5$ GeV/c, $\|\eta\| < 1$) divided by the scalar E_T sum of all particles (all p_T, $\|\eta\| < 1$)	Scalar p_T sum of "good" charged tracks ($p_T > 0.5$ GeV/c, $\|\eta\| < 1$) divided by the scalar E_T sum of calorimeter towers ($E_T > 0.1$ GeV, $\|\eta\| < 1$)
Jet Mass	Invariant mass of all particles (charged and neutral) in the jet	Invariant mass of the calorimeter jet

II. Data Selection and Track Cuts

(1) Data Selection

The data used in this analysis arise from the set of Stntuples created for the QCD group by Anwar Bhatti, Ken Hatakeyama, and Craig Group (see Table 3). Events are required to be on the "goodrun" list (version 17). They are also required to have a missing E_T significance less than 5 $GeV^{1/2}$ and to have a sumET < 1.5 TeV. We require events to have one and only one quality 12 vertex with $|z| < 60$ cm. We use the data through period 7 which corresponds to about 1.13 fb^{-1} of integrated luminosity.

Table 3. Data sets and event selection criterion used in this analysis ($L \sim 1.13$ fb^{-1}).

Event Selection	Min-Bias	JET20	JET50	JET70	JET100
Total Events	42,617,952	44,222,869	14,908,525	11,767,454	13,042,678
"Good" Events (version 7)	37,743,730	38,313,024	13,593,437	10,641,265	11,885,234
MetSig < 5 $GeV^{1/2}$, sumET < 1.5 TeV	37,742,980	38,292,213	13,474,058	10,406,781	11,029,162
1 Q12 ZVtx, $\|z\| < 60$ cm	21,883,286	16,715,344	6,104,424	4,320,713	4,604,624
"Leading Jet" $\|\eta(\text{jet}\#1) < 2\|$	6,823,559	11,862,105	5,182,183	3,939,999	4,459,757

In forming the observables in Table 2 the five trigger sets shown in Table 3 are pieced together as shown in Table 4. The lower E_T trigger set is used until it overlaps the next trigger set and then that trigger set is used until it overlaps the next trigger set etc..

Table 4. Range of P_T(jet#1 uncorrected) used for each data set.

Trigger Set	Calorimeter Jets
Min-Bias	P_T(jet#1 uncorrected) < 30 GeV
JET20	30 < P_T(jet#1 uncorrected) < 70 GeV
JET50	70 < P_T(jet#1 uncorrected) < 95 GeV
JET70	95 < P_T(jet#1 uncorrected) < 130 GeV
JET100	P_T(jet#1 uncorrected) > 130 GeV

(2) Track Cuts (Loose and Tight)

We consider only COT measured charged tracks in the region $0.5 < p_T < 150$ GeV/c and $|\eta| < 1$ where efficiency is high. The upper limit of 150 GeV/c is chosen to prevent miss-measured tracks with very high p_T from contributing to the observables in Table 2 (at high p_T the track resolution deteriorates). In addition, we employ both a "loose" and "tight" track criterion. The "loose" criterion is similar to our Run 1 analysis. For the "tight" case the transverse impact parameter is corrected for the beam position.

Table 5. Track Selection criterion, where d_0 is the transverse impact parameter and $\Delta z = z - z_{Q12}$ is the longitudinal distance between the measured track and the primary quality 12 vertex.

Track Selection (loose)	Track Selection (tight)
COT measured tracks	COT measured tracks
$\|d_0\| < 1$ cm (*not beam corrected*)	$\|d_0\| < 0.5$ cm (*beam corrected*)
$\|\Delta z\| < 3$ cm	$\|\Delta z\| < 2$ cm
NumAXseg(COT) $\geq$ 2 NumAXseg(COT) $\geq$ 2	NumAXseg(COT) $\geq$ 2 NumAXseg(COT) $\geq$ 2
NumAXhits(COT) $\geq$ 10 NumAXhits(COT) $\geq$ 10	NumAXhits(COT) $\geq$ 10 NumAXhits(COT) $\geq$ 10
χ^2(track fit)/DoF < 10	χ^2(track fit)/DoF < 10
0.5 GeV/c < p_T < 150 GeV/c	0.5 GeV/c < p_T < 150 GeV/c
$\|\eta\| < 1$	$\|\eta\| < 1$

III. Correcting the Data to the Particle Level

(1) "Response" and "Correction" Factors

We use the "one-step" method to correct the data to the particle level [7]. PYTHIA Tune A and HERWIG are used to calculate the observables in Table 2 at the particle level in bins of particle jet#1 p_T (GEN) and at the detector level in bins of calorimeter jet#1 p_T (uncorrected) (CDFSIM). The detector level data in bins of calorimeter jet#1 p_T (uncorrected) are corrected by multiplying by the QCD Monte-Carlo "correction" factor, GEN/CDFSIM, as described in Table 6. We refer to the ratio CDFSIM/GEN as the "response" factor with the "correction"

factor being the reciprocal. Smooth curves are drawn through the QCD Monte-Carlo predictions at both the generator level (GEN) and the detector level (CDFSIM) to aid in comparing the theory with the data and also to construct the "correction" factors. Fig. 7 shows an example of the fits to the Monte-Carlo results.

Table 6. PYTHIA Tune A and HERWIG are used to calculate the observables in Table 2 at the particle level in bins of particle jet#1 p_T (GEN) and at the detector level in bins of calorimeter jet#1 p_T (*uncorrected*). The detector level data in bins of calorimeter jet#1 p_T (*uncorrected*) are corrected by multiplying by QCD Monte-Carlo factor, GEN/CDFSIM.

Particle Level Observable	Detector Level Observable	"Response" Factor	"Correction" Factor
GEN = Particle Jet#1 p_T Bin	CDFSIM = Calorimeter Jet#1 p_T Bin (*uncorrected*)	CDFSIM/GEN	GEN/CDFSIM

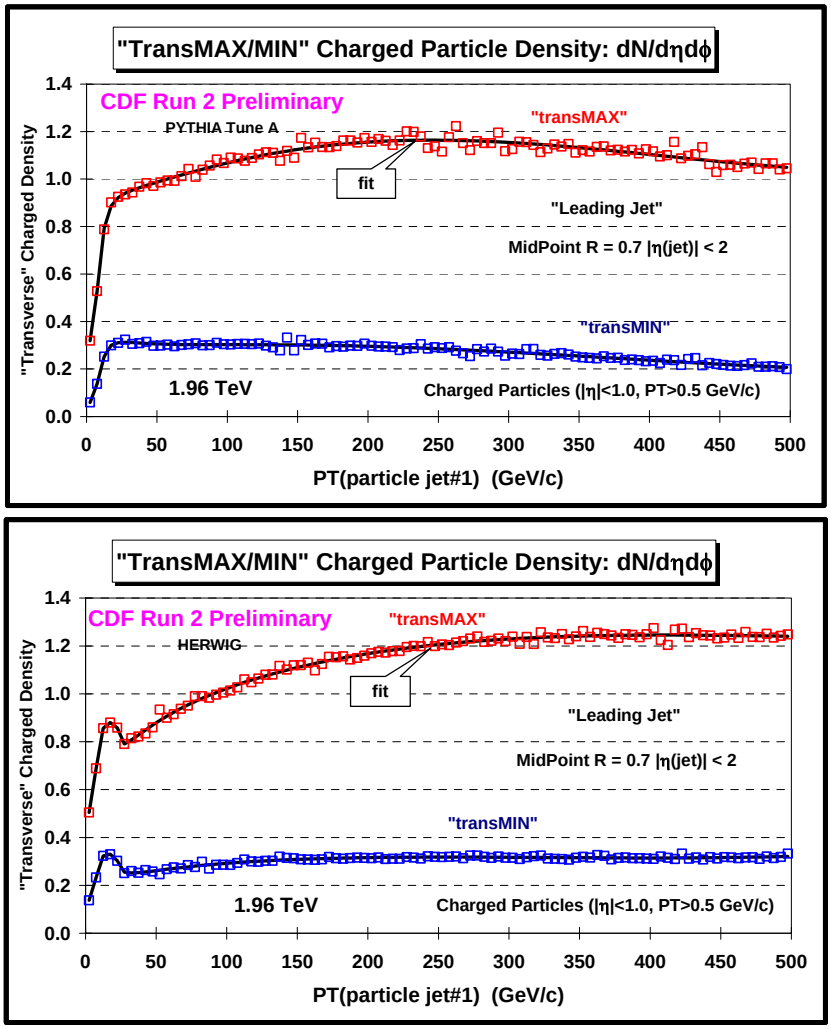

Fig. 7. Example of fits to the QCD Monte-Carlo results. Shows the particle level predictions at 1.96 TeV for the density of charged particles, dN/dηdϕ, with $p_T > 0.5$ GeV/c and $|\eta| < 1$ in the "transMAX" and "transMIN" regions for "leading jet" events as a function of the leading particle jet p_T for PYTHIA Tune A (*top*) and HERWIG (*bottom*).

(2) Systematic Uncertainty

We correct the data to the particle level in three different ways as shown in Table 7. The first way is to use the "correction" factors constructed using PYTHIA Tune A with "tight" track cuts and to apply the correction to the data with "tight" track cuts (pyA-tight). The second is to use the "correction" factors constructed with PYTHIA Tune A with "loose" track cuts and to apply the correction to the data with "loose" track cuts (pyA-loose). If PYTHIA Tune A fit the data perfectly and if CDFSIM was perfect then the corrected data from pyA-tight and pyA-loose would be identical. As shown in Table 8, the difference between pyA-tight and pyA-loose is used as one source of systematic error, σ_1. For observables that involve only the calorimeter tower energies σ_1 is identically zero and instead we take $\sigma_1 = 3\%$ to allow for uncertainty in the calorimeter response.

The third way is to use the "correction" factors constructed from HERWIG with "tight" track cuts and to apply the correction to the data with "tight" track cuts (HW-tight). PYTHIA Tune A and HERWIG do not always agree and neither fits the data perfectly. The difference between pyA-tight and HW-tight is used as another source of systematic error, σ_2. We use pyA-tight to correct the data to the particle level and then add σ_1 and σ_2 in quadrature to determine the overall systematic error. The overall systematic error is added in quadrature to the statistical error to determine the overall error.

Table 7. Three ways that the data are corrected to the particle level (see Table 6).

Name	Method to Correct the Data
pyA-tight	Use the detector level data (with tight track cuts) and PYTHIA Tune A (with tight track cuts)
pyA-loose	Use the detector level data (with loose track cuts) and PYTHIA Tune A (with loose track cuts)
HW-tight	Use the detector level data (with tight track cuts) and HERWIG (with tight track cuts)

Table 8. The errors on the corrected observables in Table 3 include both the statistical error and the systematic uncertainty (added in quadrature). The systematic uncertainty consists of σ_1 and σ_2 (added in quadrature). For observables that involve only the calorimeter tower energies $\sigma_1 \equiv 0$ and instead we take $\sigma_1 = 3\%$ to allow for uncertainty in the calorimeter response.

Uncertainty	Origin
σ_1	Bin by bin difference between the corrected data using pyA-tight and pyA-loose (see Table 7).
σ_2	Bin by bin difference between the corrected data using pyA-tight and pyA-loose (see Table 7).

(3) Examples

We will not show all the "response" factors. However, we will illustrate our technique with a few examples. Fig. 8 shows the detector level density of charged particles, $dN/d\eta d\phi$, with $p_T > 0.5$ GeV/c and $|\eta| < 1$ in the "transverse" region for "leading jet" events as a function of the leading jet p_T compared with PYTHIA Tune A and HERWIG at the "detector level" and the "particle level" . Fig. 8 also shows the "response" factor for the "transverse" charged particle

density for HW-tight and pyA-tight methods. The "response" factors for HW-tight and pyA-tight are very similar (≈ 0.9) except at small p_T(jet#1). The difference at small p_T(jet#1) is due to the fact that PHYTHIA Tune A and HERWIG behave differently in this region. HERWIG has a "bump", while PYTHIA Tune A does not. Fig. 9 shows the detector level density of charged particles in the "transverse" region for the "tight" and "loose" track cuts and also shows the "response" factor for the pyA-tight and pyA-loose methods. Fig. 10 shows the data corrected to the particle level for the density of charged in the "transverse" region for the three methods (pyA-tight, pyA-loose, HW-tight). The pyA-tight and pyA-loose methods produce nearly the same result, which indicates that PYTHIA Tune A is doing a good job modeling the data. The HW-tight and pyA-tight methods differ at small p_T(jet#1) resulting in a large systematic error in this region.

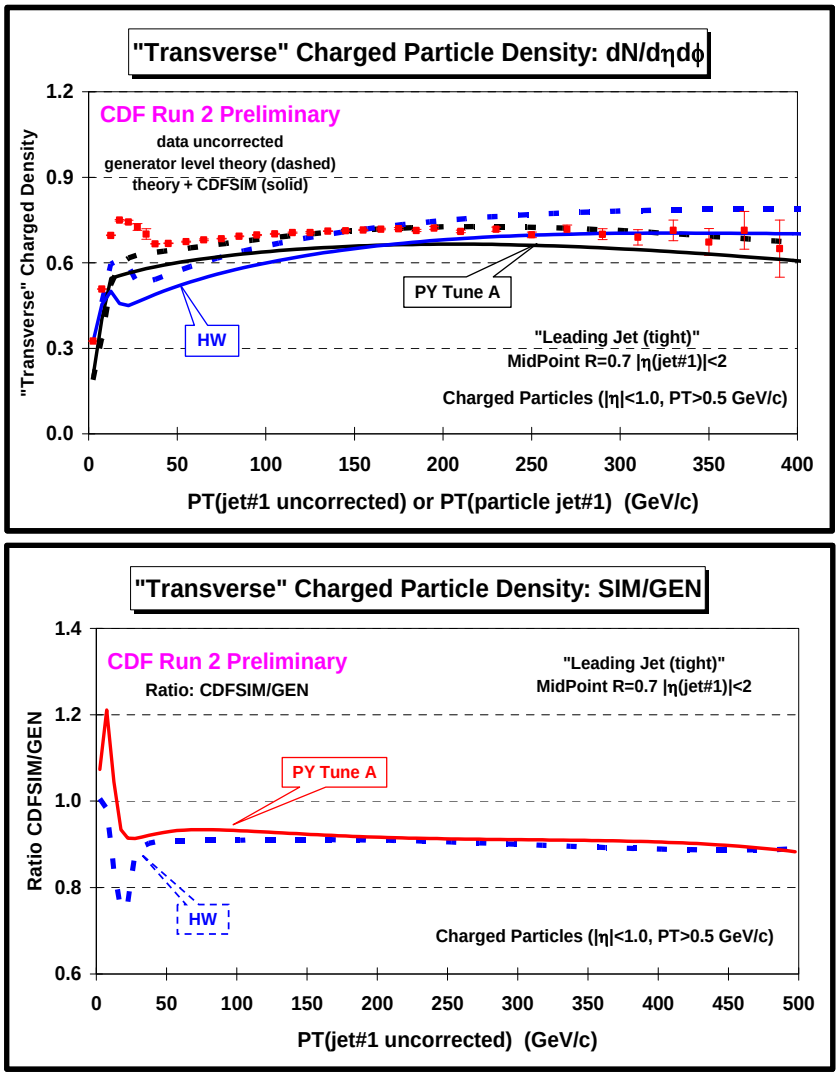

Fig. 8. (*upper*) Shows the detector level density of charged particles, dN/dηdϕ, with $p_T > 0.5$ GeV/c and $|\eta| < 1$ in the "transverse" region for "leading jet" events as a function of the leading jet p_T compared with PYTHIA Tune A and HERWIG at the "detector level" (*solid*) and the "particle level" (*dashed*). (*lower*) Shows the ratio of the detector level to the particle level, CDFSIM/GEN, versus the leading jet p_T (*i.e.* response factor) for the HW-tight and pyA-tight.

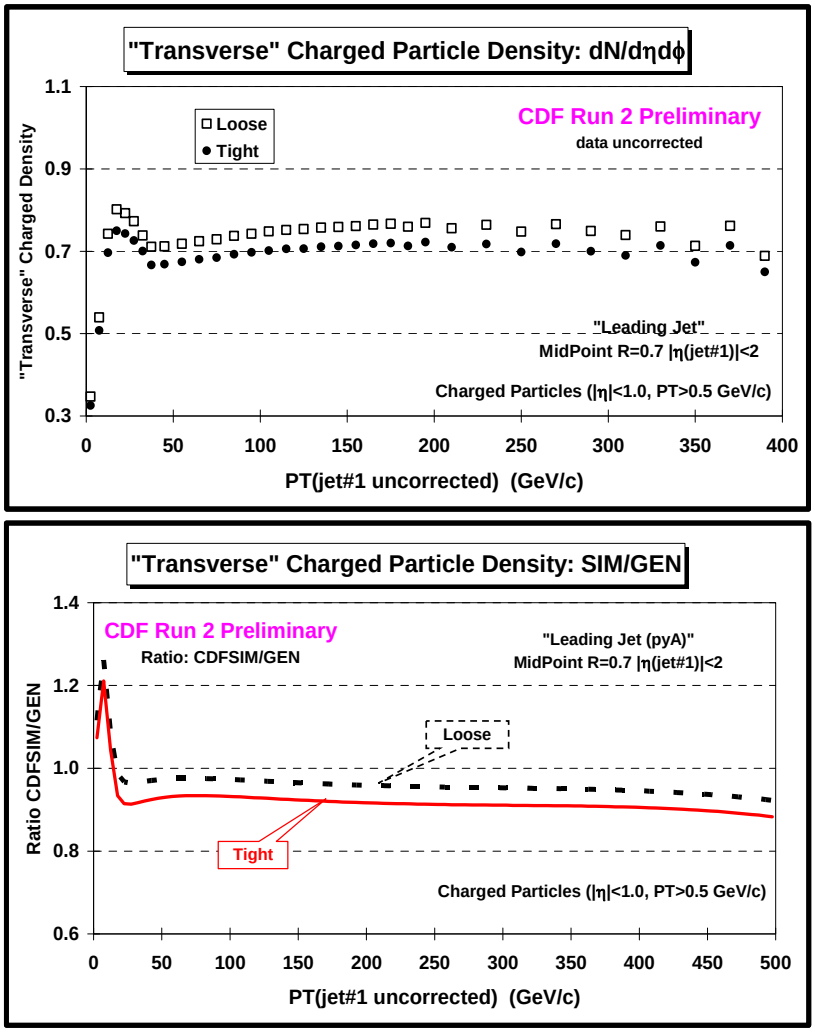

Fig. 9. (*upper*) Shows the detector level density of charged particles, dN/dηdϕ, with $p_T > 0.5$ GeV/c and $|\eta| < 1$ in the "transverse" region for "leading jet" events as a function of the leading jet p_T for the "tight" and "loose" track cuts. (*lower*) Shows the ratio of the detector level to the particle level, CDFSIM/GEN, versus the leading jet p_T (*i.e.* response factor) for the pyA-tight and pyA-loose methods.

Fig. 11 shows the detector level scalar p_T sum density of charged particles, dPT/dηdϕ, with $p_T > 0.5$ GeV/c and $|\eta| < 1$ in the "toward" region for "leading jet" events as a function of the leading jet p_T compared with PYTHIA Tune A and HERWIG at the "detector level" and the "particle level" . Fig. 11 also shows the "response" factor for the "toward" charged PTsum density for HW-tight and pyA-tight methods. Again, the "response" factors for HW-tight and pyA-tight are very similar except at small p_T(jet#1). However, unlike the "transverse" region, the "response" factor becomes small at large p_T(jet#1). At 450 GeV/c the "correction" factor is about a factor of two. This is a manifestation of our track selection of $0.5 < p_T < 150$ GeV/c (see table 5). The Mone-Carlo is correcting back for the "true" particles that were lost by requiring $p_T < 150$ GeV/c. Fig. 12 shows the detector level PTsum density in the "toward" region for the "tight" and "loose" track cuts and also shows the "response" factor for the pyA-tight and pyA-loose methods. Fig. 13 shows the data corrected to the particle level for the density of charged in the "toward" region for the three methods (pyA-tight, pyA-loose, HW-tight). All three methods produce nearly the same result.

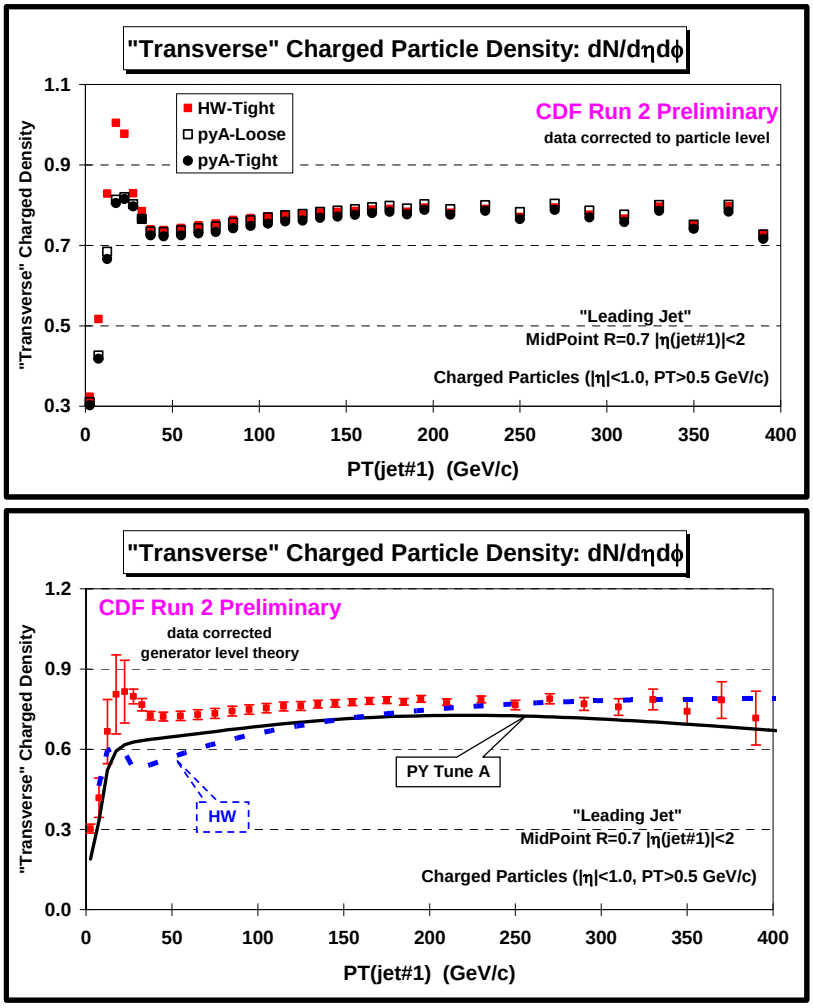

Fig. 10. (*upper*) Shows the data corrected to the particle level for the density of charged particles, $dN/d\eta d\phi$, with $p_T > 0.5$ GeV/c and $|\eta| < 1$ in the "transverse" region for "leading jet" events as a function of the leading jet p_T for the three methods given in Table X (pyA-tight, pyA-loose, HW-tight). (*lower*) Data at 1.96 TeV on the density of charged particles, $dN/d\eta d\phi$, with $p_T > 0.5$ GeV/c and $|\eta| < 1$ in the "transverse" regions for "leading jet" events as a function of the leading jet p_T compared with PYTHIA Tune A and HERWIG. The data are corrected to the particle level (with errors that include both the statistical error and the systematic uncertainty) and are compared with the theory at the particle level (*i.e.* generator level).

Fig. 14 and Fig. 15 show the "response" factors for the "transverse" energy density and for the leading jet mass, respectively. The "response" factors for the "transverse" energy and the leading jet mass are similar. They are small at small p_T(jet#1) and about 0.7 at high p_T(jet#1), resulting in large corrections for p_T(jet#1) < 50 GeV/c and corrections of around 40% at high p_T(jet#1). Because the COT and the calorimeter responds differently to particles, the "response" factor for the "transverse" charged fraction, PTsum/ETsum, is greater than one and large. As can be seen in Fig. 16, the "response" factor for the "transverse" charged fraction is around 1.7 at high p_T(jet#1). The charged PTsum is measured fairly accurately by the COT, while the calorimeter sees only a small fraction of the true ETsum, resulting in a "correction" factor of around 0.6 at high p_T(jet#1).

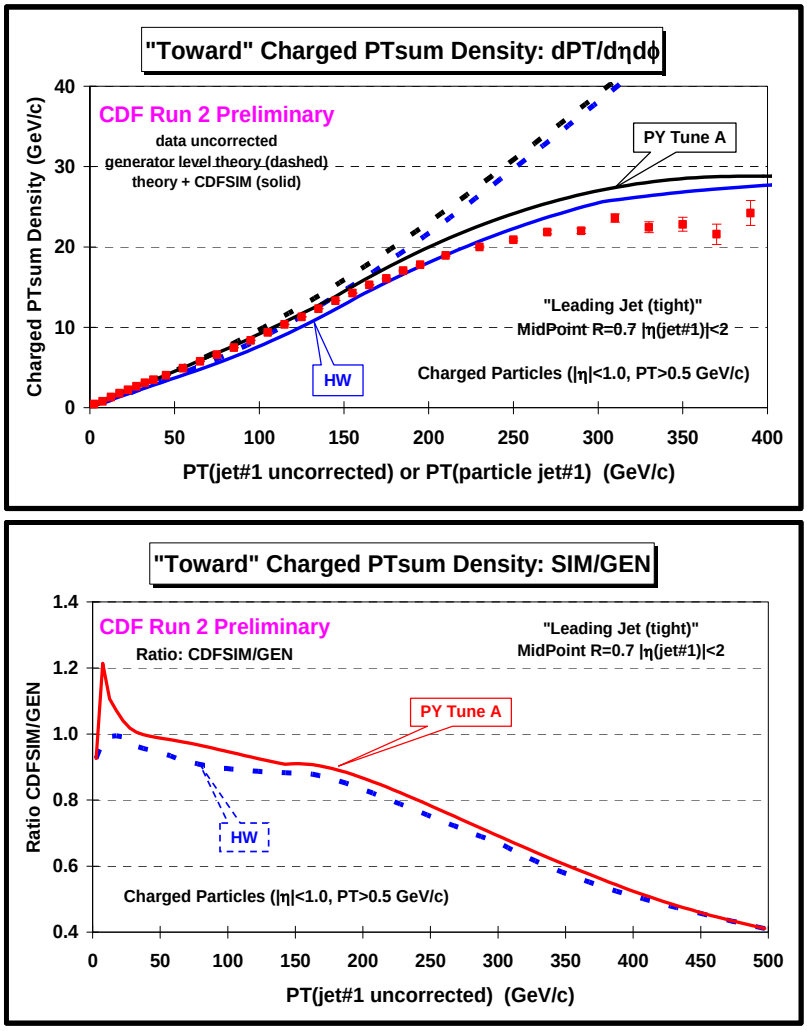

Fig. 11. (*upper*) Shows the detector level PTsum density of charged particles, dPT/dηdϕ, with $p_T > 0.5$ GeV/c and $|\eta| < 1$ in the "toward" region for "leading jet" events as a function of the leading jet p_T compared with PYTHIA Tune A and HERWIG at the "detector level" (*solid*) and the "particle level" (*dashed*). (*lower*) Shows the ratio of the detector level to the particle level, CDFSIM/GEN, versus the leading jet p_T (*i.e.* response factor) for the HW-tight and pyA-tight methods.

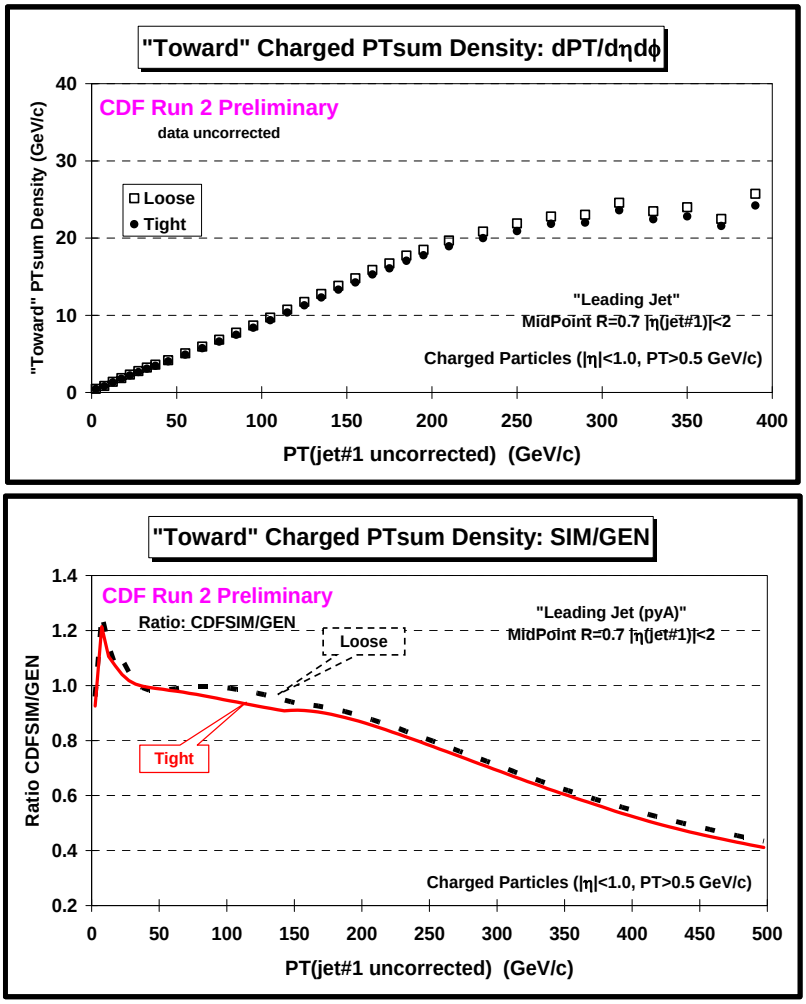

Fig. 12. (*upper*) Shows the detector level PTsum density of charged particles, dPT/dηdϕ, with $p_T > 0.5$ GeV/c and $|\eta| < 1$ in the "toward" region for "leading jet" events as a function of the leading jet p_T for the "tight" and "loose" track cuts. (*lower*) Shows the ratio of the detector level to the particle level, CDFSIM/GEN, versus the leading jet p_T (*i.e.* response factor) for the pyA-tight and pyA-loose methods.

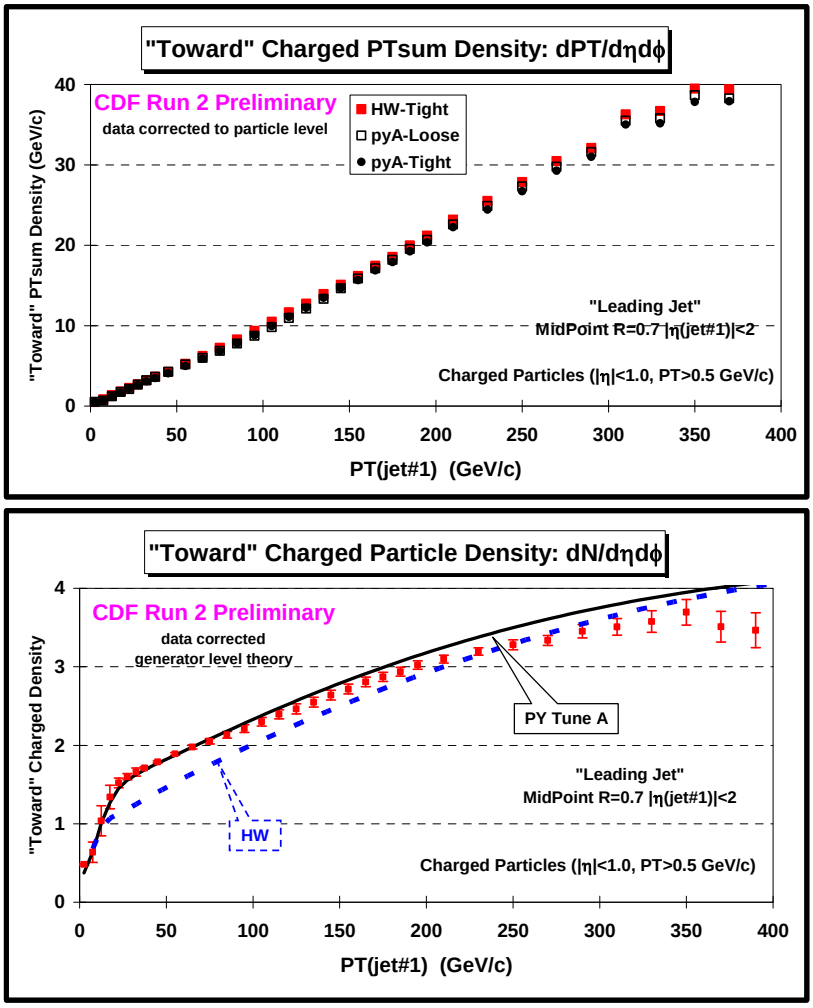

Fig. 13. (*upper*) Shows the data corrected to the particle level for the charged PTsum density, dPT/dηdϕ, with $p_T > 0.5$ GeV/c and $|\eta| < 1$ in the "toward" region for "leading jet" events as a function of the leading jet p_T for the three methods given in Table X (pyA-tight, pyA-loose, HW-tight). (*lower*) Data at 1.96 TeV on the charged PTsum density, dPT/dηdϕ, with $p_T > 0.5$ GeV/c and $|\eta| < 1$ in the "toward" regions for "leading jet" events as a function of the leading jet p_T compared with PYTHIA Tune A and HERWIG. The data are corrected to the particle level (with errors that include both the statistical error and the systematic uncertainty) and are compared with the theory at the particle level (*i.e.* generator level).

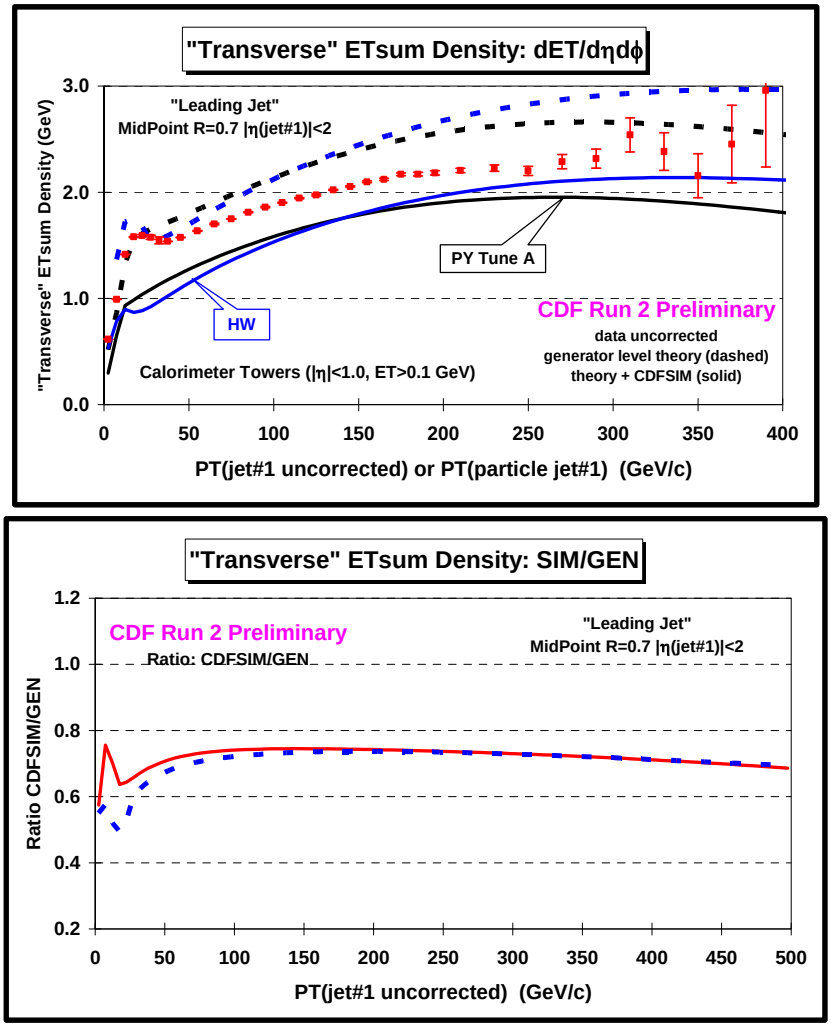

Fig. 14. (*upper*) Shows the detector level ETsum density, dET/dηdϕ, with |η| < 1 in the "transverse" region for "leading jet" events as a function of the leading jet p_T compared with PYTHIA Tune A and HERWIG at the "detector level" (*solid*) and the "particle level" (*dashed*). (*lower*) Shows the ratio of the detector level to the particle level, CDFSIM/GEN, versus the leading jet p_T (*i.e.* response factor) for HERWIG and PYTHIA Tune A.

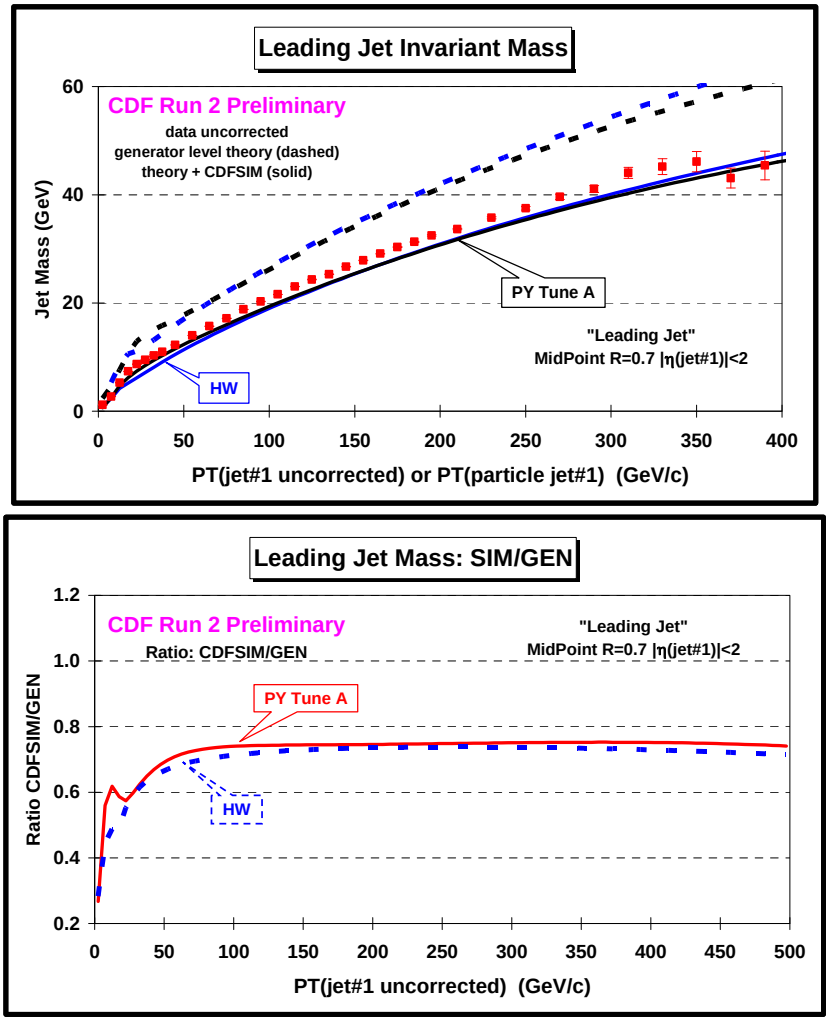

Fig. 15. (*upper*) Shows the leading jet mass at the detector level for "leading jet" events as a function of the leading jet p_T compared with PYTHIA Tune A and HERWIG at the "detector level" (*solid*) and the "particle level" (*dashed*). (*lower*) Shows the ratio of the detector level to the particle level, CDFSIM/GEN, versus the leading jet p_T (*i.e.* response factor) for HERWIG and PYTHIA Tune A.

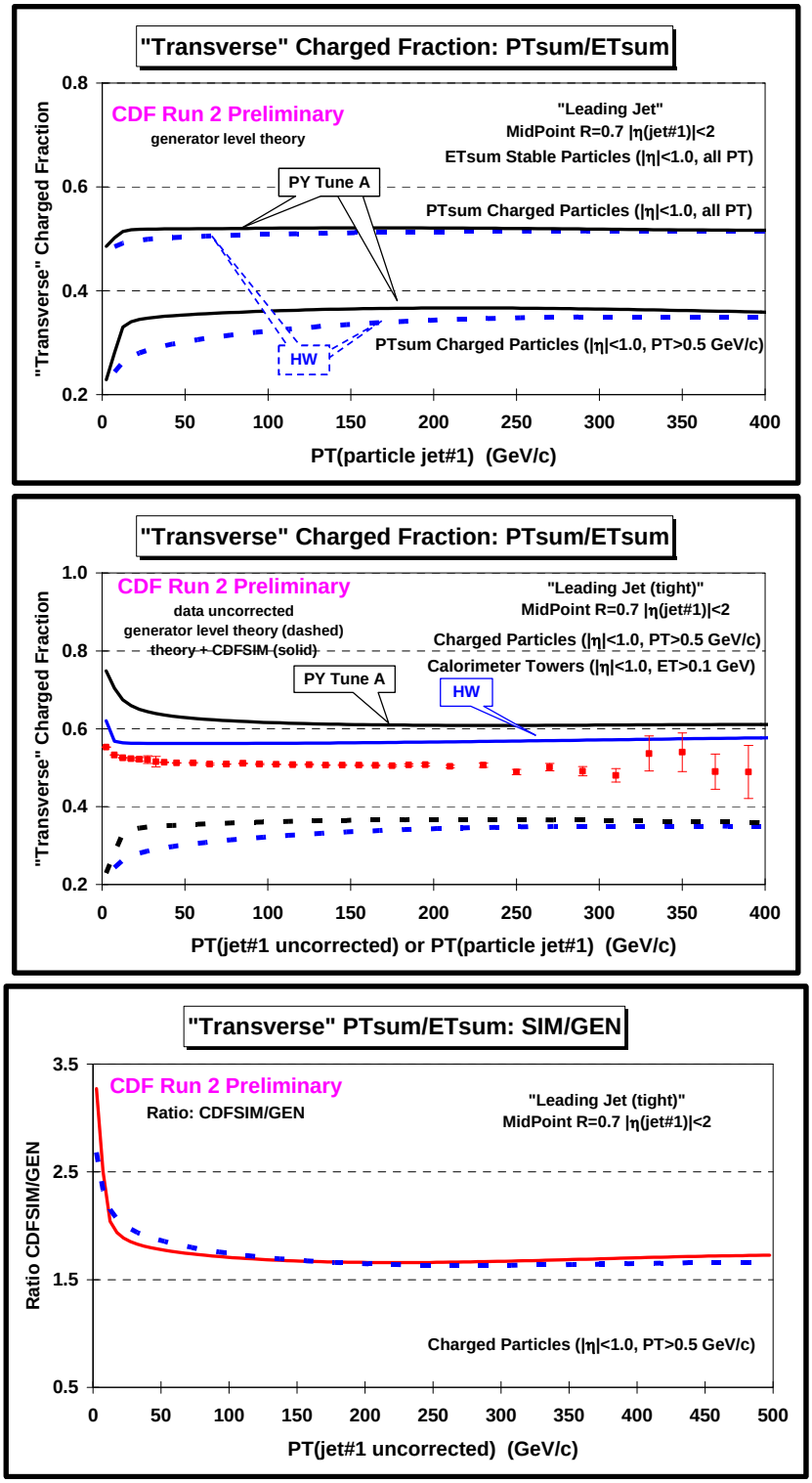

Fig. 16. (*upper*) Shows the generator level "transverse" charged fraction, PTsum/ETsum, for PYTHIA Tune A and HERWIG. The upper two curves correspond to the ratio of the PTsum of all charged particles (all pT, $|\eta| < 1$) to the ETsum of all stable particles (all p_T, $|\eta| < 1$), while the lower two curves correspond to the ratio of the PTsum of charged particles ($p_T < 0.5$ GeV/c, $|\eta| < 1$) to the ETsum of all stable particles (all p_T, $|\eta| < 1$) . (*middle*) Shows the detector level "transverse" charged fraction, PTsum($p_T > 0.5$, $|\eta|<1$)/ETsum($|\eta| < 1$), for "leading jet" events as a function of the leading jet p_T compared with PYTHIA Tune A and HERWIG at the "detector level" (*solid*) and the "particle level" (*dashed*). (*lower*) Shows the ratio of the detector level to the particle level, CDFSIM/GEN, versus the leading jet p_T (*i.e.* response factor) for the HW-tight and pyA-tight methods.

IV. The "Leading Jet" Results

(1) Overall Region

The overall region is the sum of the "toward", "away", and "transverse" regions. Fig. 17 and Fig. 18 show the data at 1.96 TeV on the overall number of charged particles ($p_T > 0.5$ GeV/c, $|\eta| < 1$) and the overall *scalar* p_T sum of charged particles ($p_T > 0.5$ GeV/c, $|\eta| < 1$) and the overall *scalar* E_T sum of all particles ($|\eta| < 1$) for "leading jet" events as a function of the leading jet p_T. The data are corrected to the particle level (with errors that include both the statistical error and the systematic uncertainty) and are compared with PYTHIA Tune A (with multiple parton interactions) and HERWIG (without multiple parton interactions) at the particle level (*i.e.* generator level). HERWIG produces too few particles at low p_T(jet#1) and both HERWIG and PYTHIA Tune A produce too much PTsum at large p_T(jet#1).

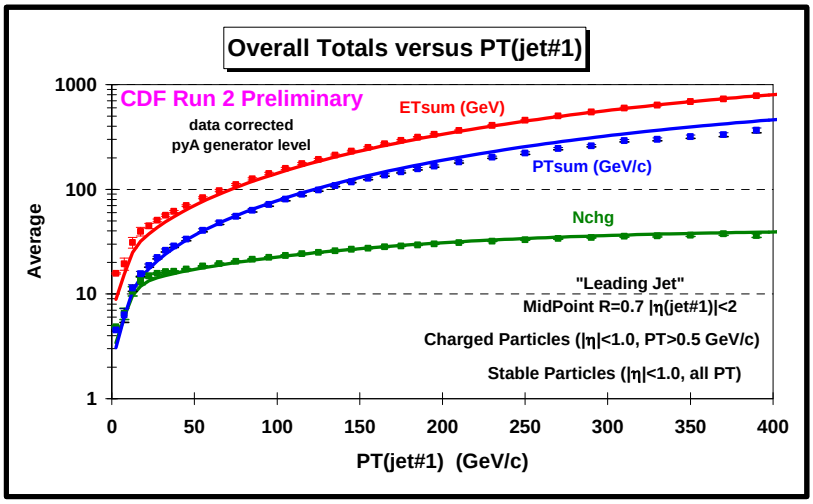

Fig. 17. Data at 1.96 TeV on the overall number of charged particles ($p_T > 0.5$ GeV/c, $|\eta| < 1$) and the overall *scalar* p_T sum of charged particles ($p_T > 0.5$ GeV/c, $|\eta| < 1$) and the overall *scalar* E_T sum of all particles ($|\eta| < 1$) for "leading jet" events as a function of the leading jet p_T. The data are corrected to the particle level (with errors that include both the statistical error and the systematic uncertainty) and are compared with PYTHIA Tune A at the particle level (*i.e.* generator level).

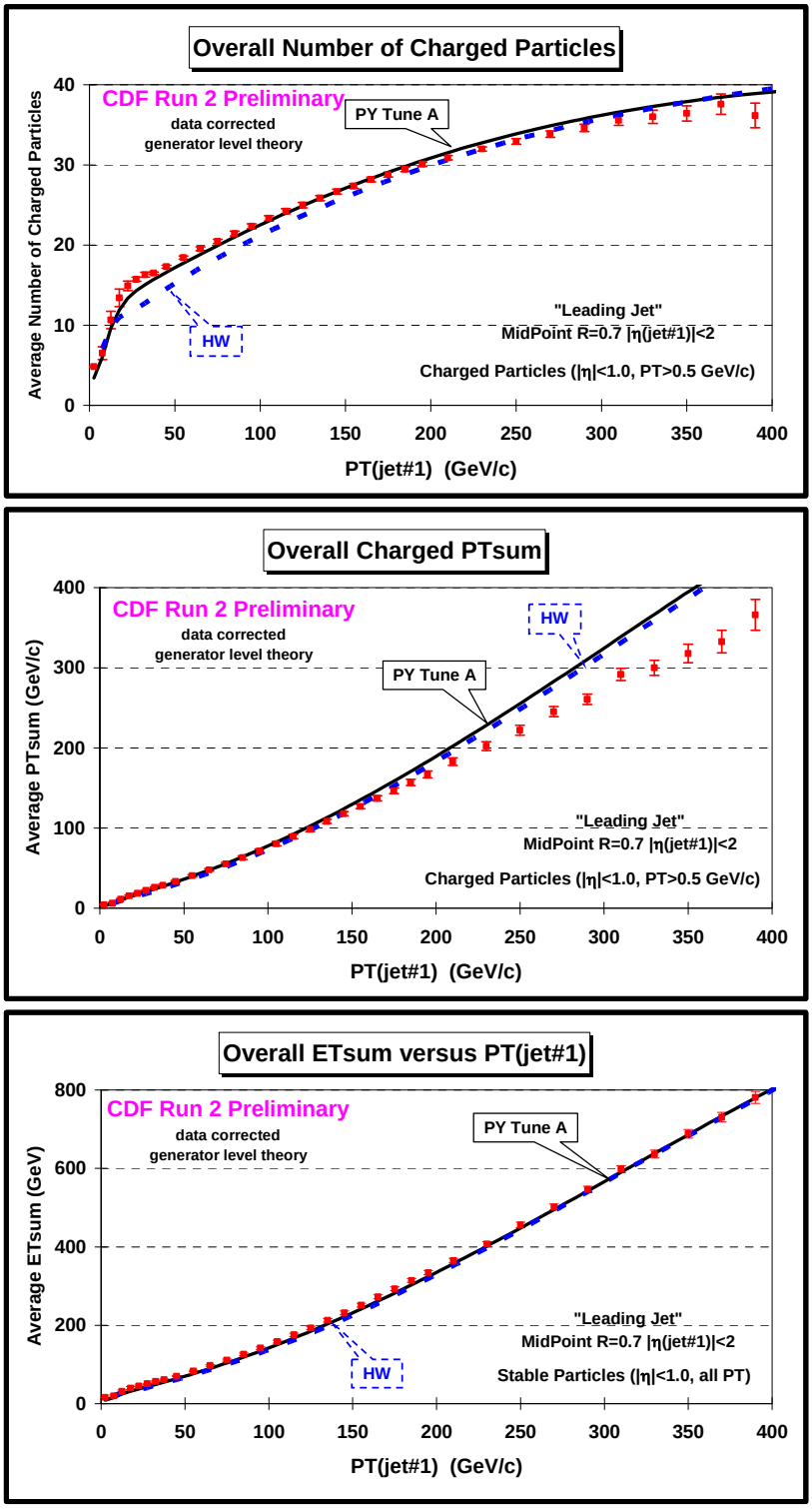

Fig. 18. Data at 1.96 TeV on the overall number of charged particles ($p_T > 0.5$ GeV/c, $|\eta| < 1$) (*top*) and the overall *scalar* p_T sum of charged particles ($p_T > 0.5$ GeV/c, $|\eta| < 1$) (*middle*) and the overall *scalar* E_T sum of all particles ($|\eta| < 1$) (*bottom*) for "leading jet" events as a function of the leading jet p_T. The data are corrected to the particle level (with errors that include both the statistical error and the systematic uncertainty) and are compared with PYTHIA Tune A (with multiple parton interactions) and HERWIG (without multiple parton interactions) at the particle level (*i.e.* generator level).

(2) The Leading jet Mass

Fig. 19 shows the corrected data at 1.96 TeV on the leading jet mass for "leading jet" events as a function of the leading jet p_T compared with PYTHIA Tune A (with multiple parton interactions) and HERWIG (without multiple parton interactions) at the particle level (*i.e.* generator level). Both PYTHIA Tune A and HERWIG are low by a few GeV on the leading jet mass.

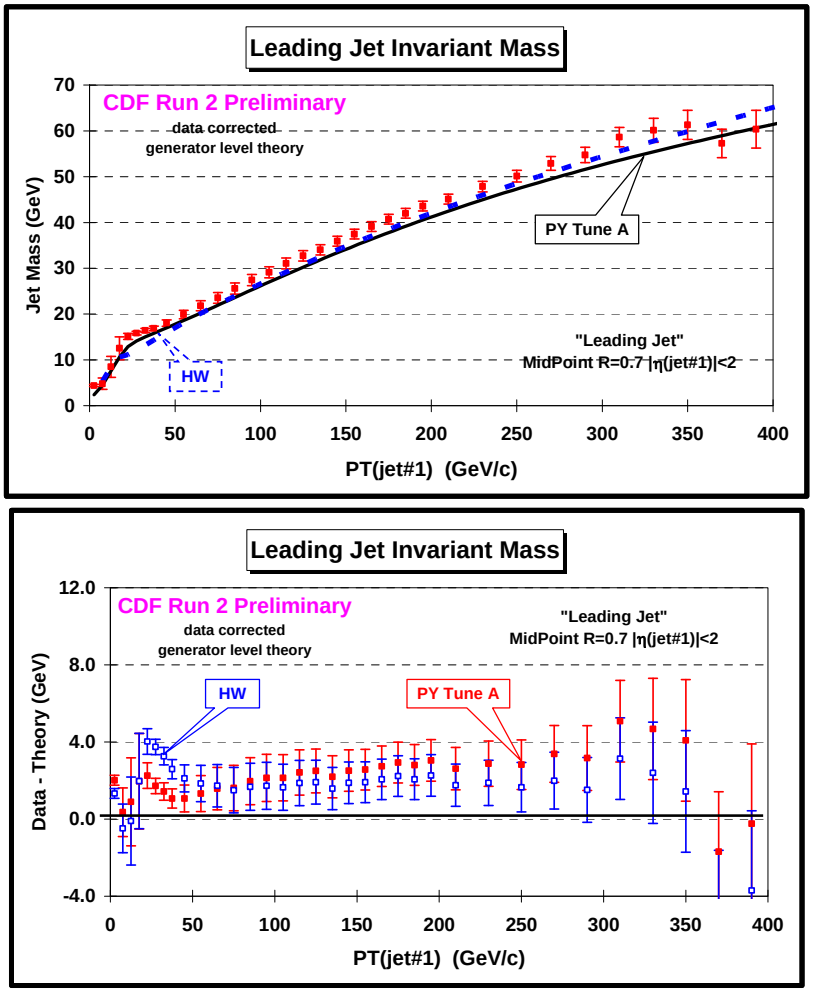

Fig. 19. (*top*) Data at 1.96 TeV on the leading jet mass for "leading jet" events as a function of the leading jet p_T. The data are corrected to the particle level (with errors that include both the statistical error and the systematic uncertainty) and are compared with PYTHIA Tune A (with multiple parton interactions) and HERWIG (without multiple parton interactions) at the particle level (*i.e.* generator level). (*bottom*) Shows the data minus the theory for PYTHIA Tune A (with multiple parton interactions) and HERWIG (without multiple parton interactions).

(3) The "Toward", "Away", and "Transverse" Region

Fig. 20 shows the corrected data at 1.96 TeV on the density of charged particles, the charged particle *scalar* p_T sum density, and the *scalar* E_T sum density for "leading jet" events as a function of the leading jet p_T for the "toward", "away", and "transverse" regions compared

with PYTHIA Tune A at the particle level (*i.e.* generator level). PYTHIA Tune A does not have quite enough activity in the "transverse" region.

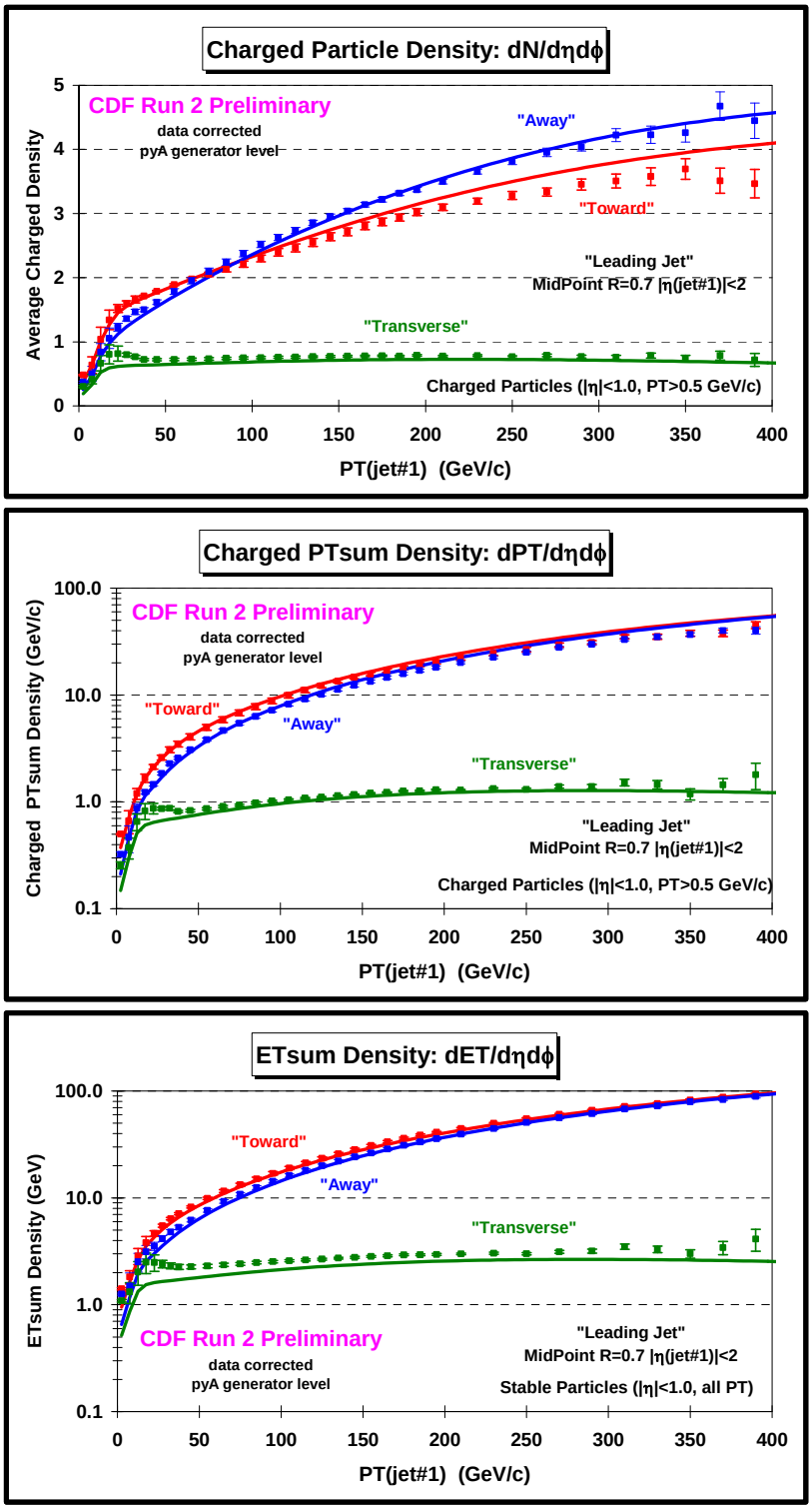

Fig. 20. Data at 1.96 TeV on the density of charged particles, $dN/d\eta d\phi$, with $p_T > 0.5$ GeV/c and $|\eta| < 1$ (*top*), and the charged particle *scalar* p_T sum density, $dPT/d\eta d\phi$, with $p_T > 0.5$ GeV/c and $|\eta| < 1$ (*middle*), and the *scalar* E_T sum density, $dET/d\eta d\phi$, of all particles with $|\eta| < 1$ (*bottom*) for "leading jet" events as a function of the leading jet p_T for the "toward", "away", and

"transverse" regions. The data are corrected to the particle level (with errors that include both the statistical error and the systematic uncertainty) and are compared with PYTHIA Tune A at the particle level (*i.e.* generator level).

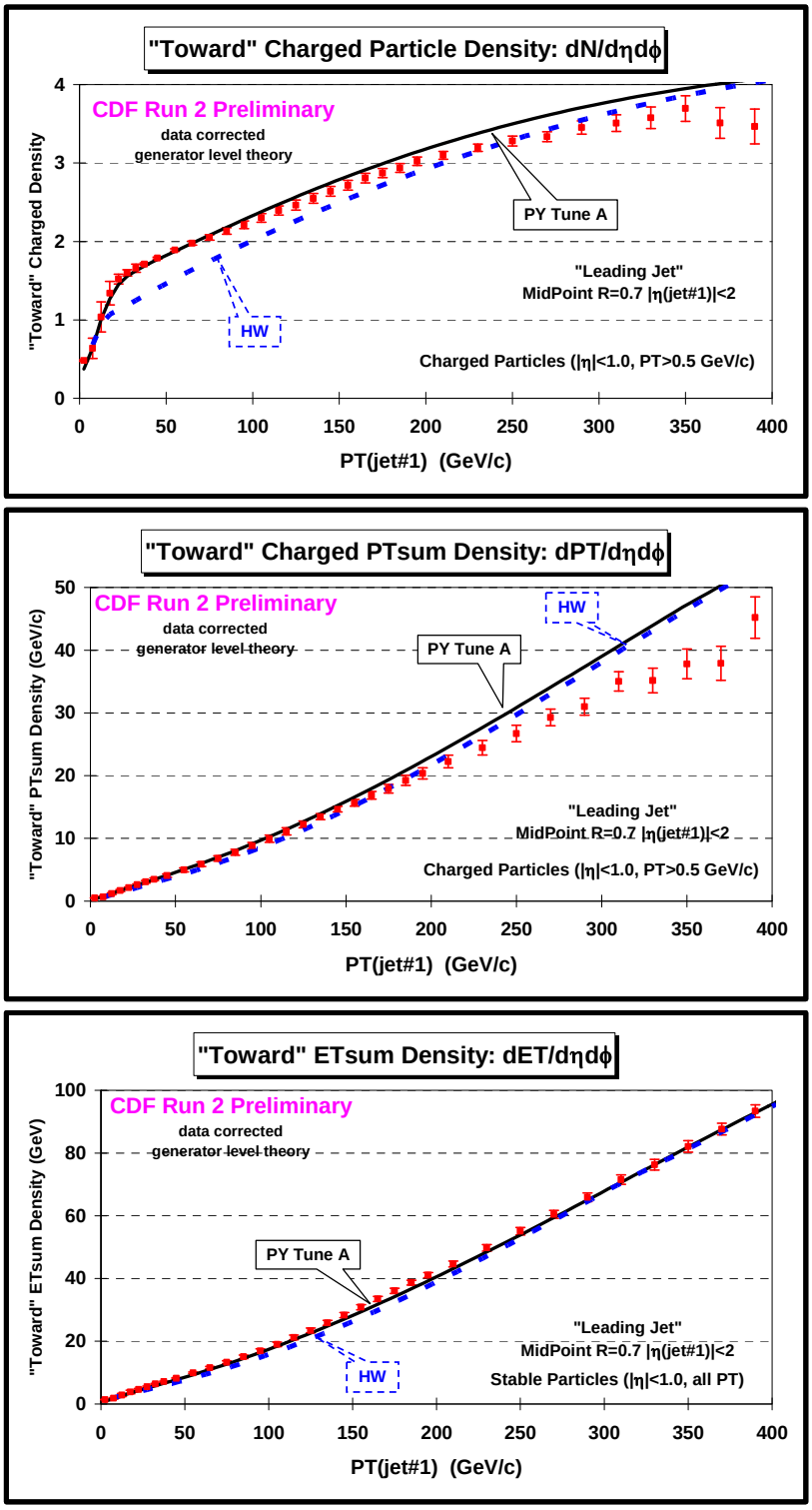

Fig. 21. Data at 1.96 TeV on the density of charged particles, $dN/d\eta d\phi$, with $p_T > 0.5$ GeV/c and $|\eta| < 1$ (*top*), and the charged particle *scalar* p_T sum density, $dPT/d\eta d\phi$, with $p_T > 0.5$ GeV/c and $|\eta| < 1$ (*middle*), and the *scalar* E_T sum density, $dET/d\eta d\phi$, of all particles with $|\eta| < 1$ (*bottom*) for the "toward" region of "leading jet" events as a function of the leading jet p_T. The data are corrected to the particle level (with errors that include both the statistical error and the systematic uncertainty) and are compared

with PYTHIA Tune A (with multiple parton interactions) and HERWIG (without multiple parton interactions) at the particle level (*i.e.* generator level).

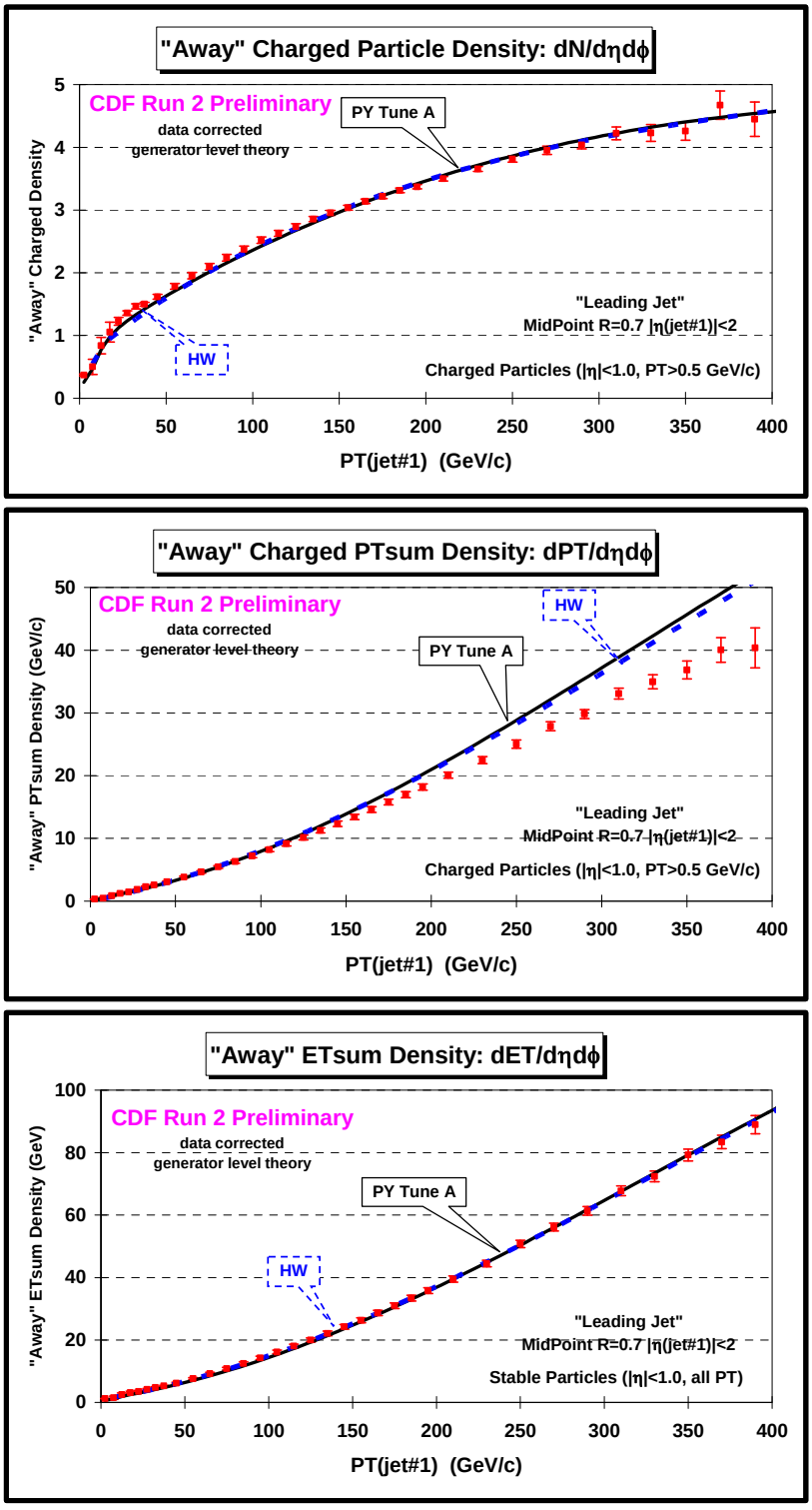

Fig. 22. Data at 1.96 TeV on the density of charged particles, $dN/d\eta d\phi$, with $p_T > 0.5$ GeV/c and $|\eta| < 1$ (*top*), and the charged particle *scalar* p_T sum density, $dPT/d\eta d\phi$, with $p_T > 0.5$ GeV/c and $|\eta| < 1$ (*middle*), and the *scalar* E_T sum density, $dET/d\eta d\phi$, of all particles with $|\eta| < 1$ (*bottom*) for the "away" region of "leading jet" events as a function of the leading jet p_T. The data are corrected to the particle level (with errors that include both the statistical error and the systematic uncertainty) and are compared

with PYTHIA Tune A (with multiple parton interactions) and HERWIG (without multiple parton interactions) at the particle level (*i.e.* generator level).

(4) The "Toward" Region

Fig. 21 shows the corrected data at 1.96 TeV on the density of charged particles, the charged particle *scalar* p_T sum density, and the *scalar* E_T sum density for "leading jet" events as a function of the leading jet p_T for the "toward" region compared with PYTHIA Tune A (with multiple parton interactions) and HERWIG (without multiple parton interactions) at the particle level (*i.e.* generator level). HERWIG produces too few charged particles at low p_T(jet#1) and both HERWIG and PYTHIA Tune A produce too much PTsum at large p_T(jet#1).

(5) The "Away" Region

Fig. 22 shows the corrected data at 1.96 TeV on the density of charged particles, the charged particle *scalar* p_T sum density, and the *scalar* E_T sum density for "leading jet" events as a function of the leading jet p_T for the "away" region compared with PYTHIA Tune A (with multiple parton interactions) and HERWIG (without multiple parton interactions) at the particle level (*i.e.* generator level). Here HERWIG and PYTHIA produce enough charged particles, but again both produce too much PTsum at large p_T(jet#1).

(6) The "Transverse" Region

Fig. 23 shows the corrected data at 1.96 TeV on the density of charged particles, the charged particle *scalar* p_T sum density, and the *scalar* E_T sum density for "leading jet" events as a function of the leading jet p_T for the "transverse" region compared with PYTHIA Tune A (with multiple parton interactions) and HERWIG (without multiple parton interactions) at the particle level (*i.e.* generator level). PYTHIA Tune A does a better job describing the data than does HERWIG, however, neither produce enough activity in the "transverse" region.

Fig. 24 shows the data minus theory for the density of charged particles, the charged particle *scalar* p_T sum density, and the *scalar* E_T sum density for the "transverse" region of "leading jet" events as a function of the leading jet p_T. At around 100 GeV/c PYTHIA Tune A predicts a charged particle density that is low by about 0.1. This corresponds, on the average, to roughly 0.42 charged particles (with $p_T > 0.5$ GeV/c) in the entire "transverse" region. Also, at around 100 GeV/c PYTHIA Tune A produces a charged PTsum density that is low by about 0.1 GeV/c, which corresponds, on the average, to roughly 420 MeV/c in the entire "transverse" region. On the other hand, at around 100 GeV/c PYTHIA Tune A predicts an ETsum density that is low by about 0.4 GeV, which corresponds, on the average, to roughly 1.7 GeV in the entire "transverse" region. Remember, however, PTsum is constructed from charged particles with $p_T > 0.5$ GeV, while ETsum includes all stable particles (all p_T).

Fig. 25 shows the corrected data for average p_T of charged particles and average maximum p_T charged particle, PTmax, for the "transverse" region of "leading jet" events as a function of the leading jet p_T compared with PYTHIA Tune A (with multiple parton interactions) and HERWIG (without multiple parton interactions) at the particle level (*i.e.* generator level). In constructing the "transverse" average p_T and "transverse" PTmax we require at least one charged

particle (p_T > 0.5 GeV/c, |η| < 1) in the "transverse" region. Here PYTHIA Tune A does a much better job in describing the data. HERWIG produces a p_T distribution of charged particles that is too "soft".

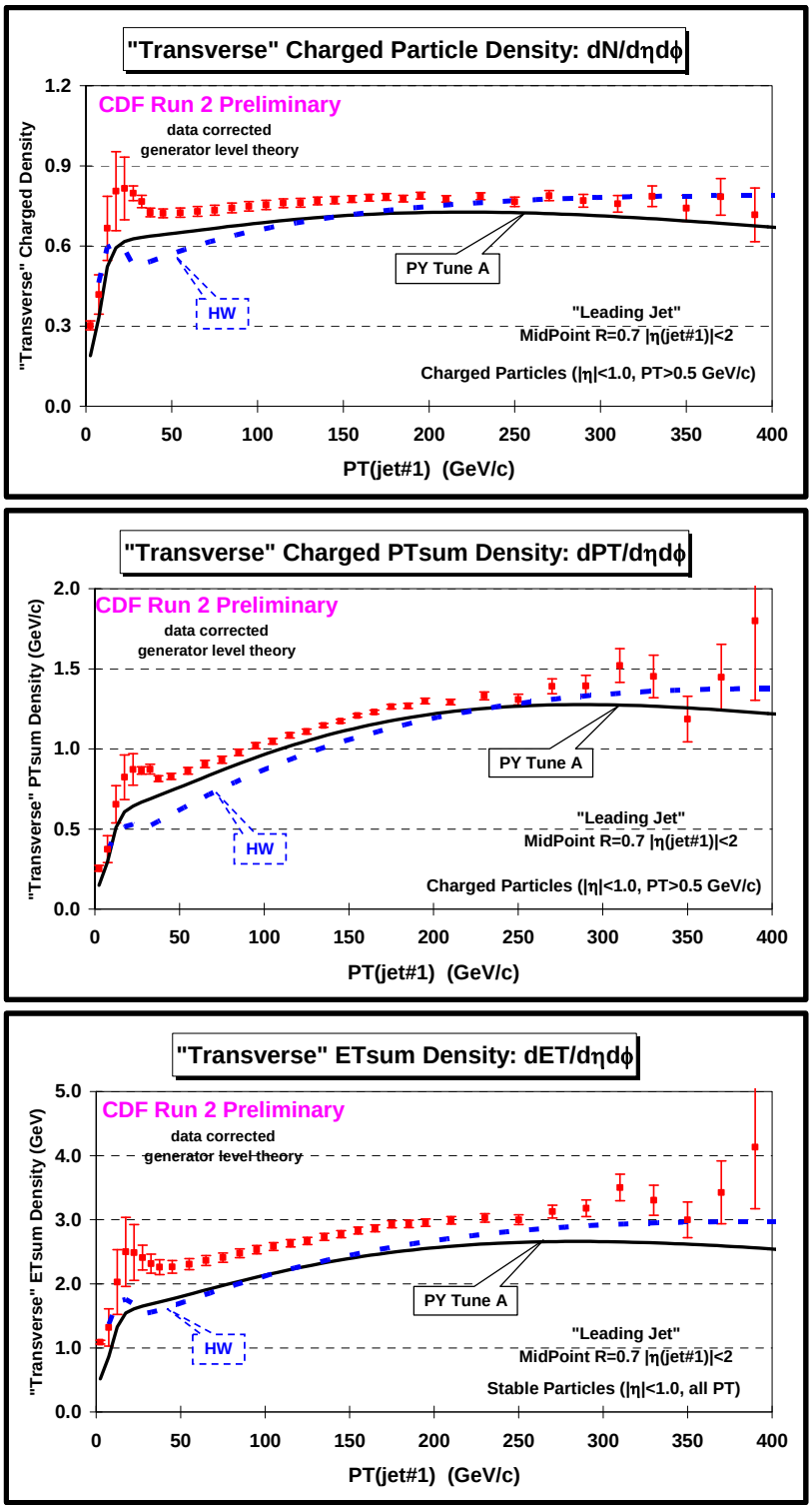

Fig. 23. Data at 1.96 TeV on the density of charged particles, dN/dηdϕ, with p_T > 0.5 GeV/c and |η| < 1 (*top*), and the charged particle *scalar* p_T sum density, dPT/dηdϕ, with p_T > 0.5 GeV/c and |η| < 1 (*middle*), and the *scalar* E_T sum density, dET/dηdϕ, of

all particles with $|\eta| < 1$ (*bottom*) for the "transverse" region of "leading jet" events as a function of the leading jet p_T. The data are corrected to the particle level (with errors that include both the statistical error and the systematic uncertainty) and are compared with PYTHIA Tune A (with multiple parton interactions) and HERWIG (without multiple parton interactions) at the particle level (*i.e.* generator level).

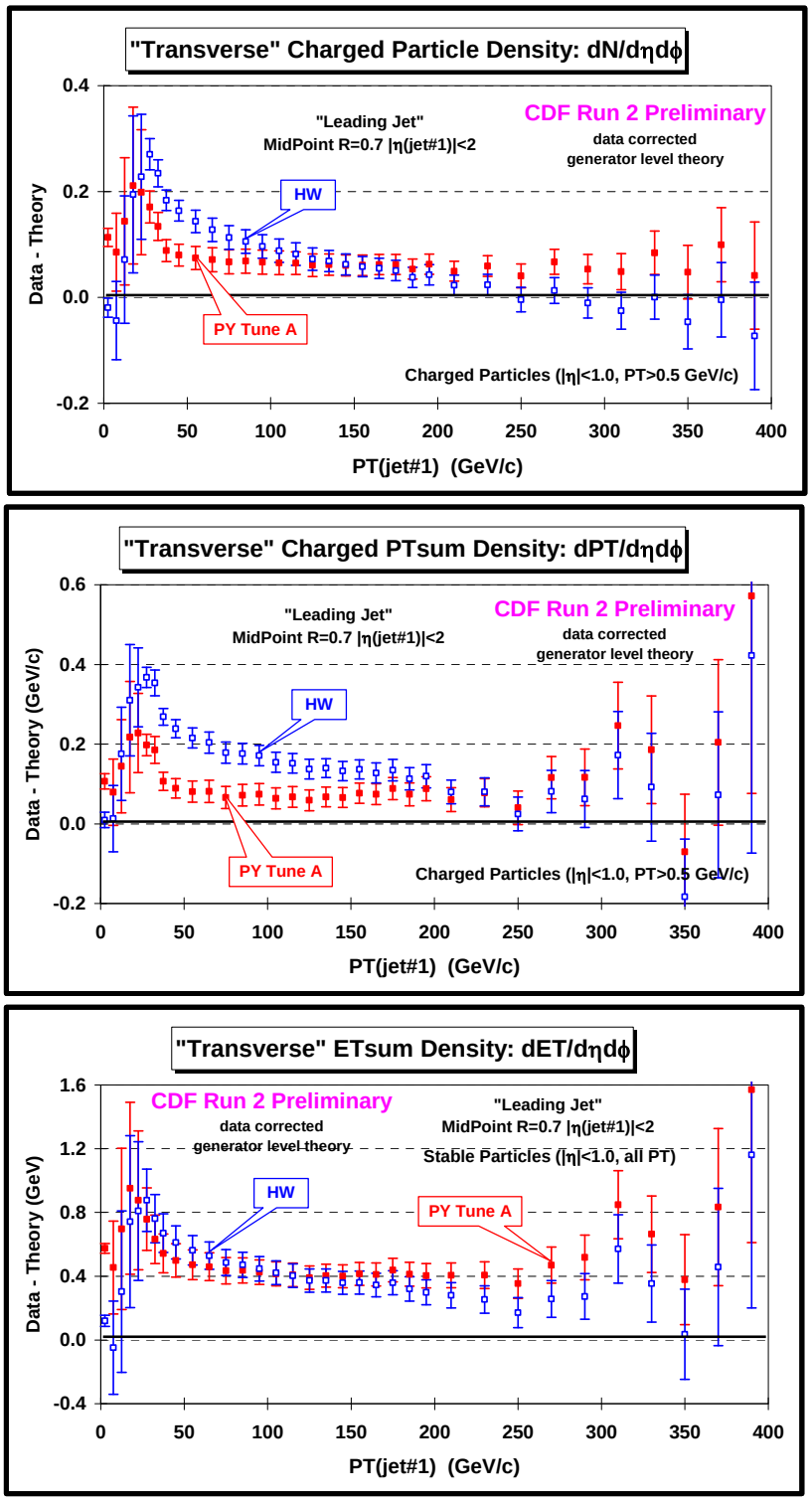

Fig. 24. Data minus theory for the density of charged particles, $dN/d\eta d\phi$, with $p_T > 0.5$ GeV/c and $|\eta| < 1$ (*top*), and the charged particle *scalar* p_T sum density, $dPT/d\eta d\phi$, with $p_T > 0.5$ GeV/c and $|\eta| < 1$ (*middle*), and the *scalar* E_T sum density, $dET/d\eta d\phi$, of

all particles with $|\eta| < 1$ (*bottom*) for the "transverse" region of "leading jet" events as a function of the leading jet p_T. The data are corrected to the particle level (with errors that include both the statistical error and the systematic uncertainty) and are compared with PYTHIA Tune A (with multiple parton interactions) and HERWIG (without multiple parton interactions) at the particle level (*i.e.* generator level).

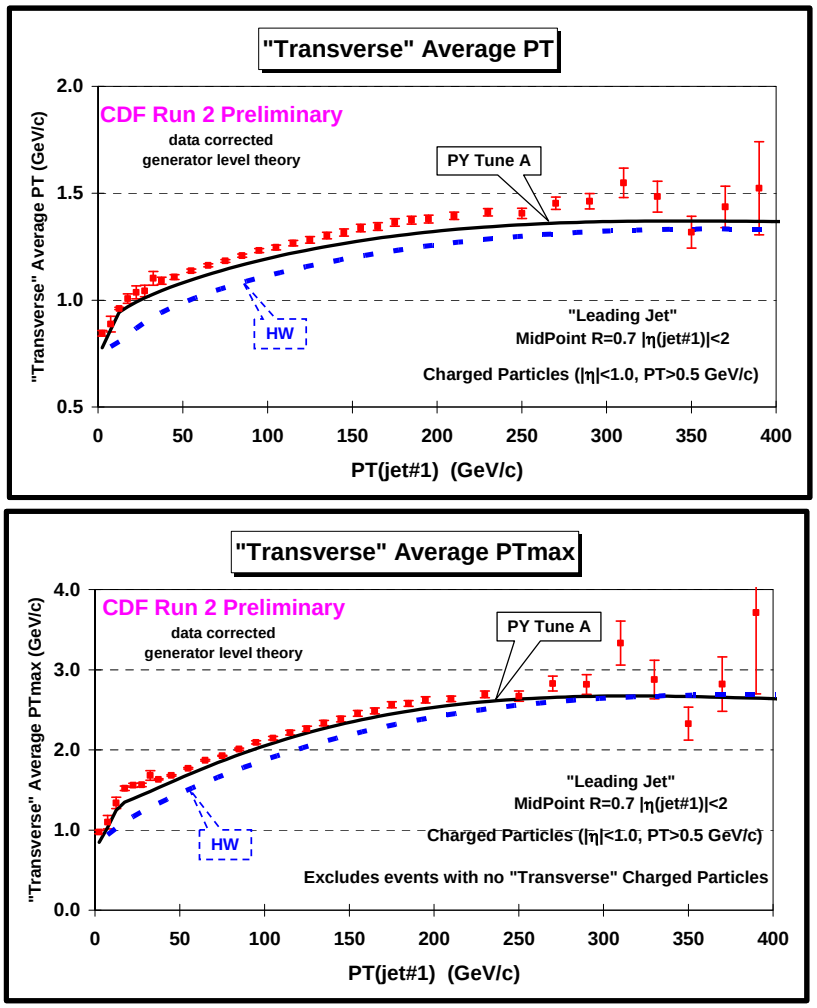

Fig. 25. Data at 1.96 TeV average p_T of charged particles with $p_T > 0.5$ GeV/c and $|\eta| < 1$ (*top*) and average maximum p_T charged particle, PTmax, with $p_T > 0.5$ GeV/c and $|\eta| < 1$ (*bottom*) for the "transverse" region of "leading jet" events as a function of the leading jet p_T. In constructing the average p_T and PTmax we require at least one charged particle ($p_T > 0.5$ GeV/c, $|\eta| < 1$) in the "transverse" region. The data are corrected to the particle level (with errors that include both the statistical error and the systematic uncertainty) and are compared with PYTHIA Tune A (with multiple parton interactions) and HERWIG (without multiple parton interactions) at the particle level (*i.e.* generator level).

(7) The "MAX/MIN Transverse" Regions

As shown in Fig. 5 we use the direction of the highest p_T jet, jet#1, to define the two "transverse" regions, $60^o < |\Delta\phi| < 120^o$ and $60^o < -|\Delta\phi| < 120^o$. On an event-by-event basis, we define "transMAX" and "transMIN" to be the maximum and minimum of these two regions. "TransMAX" and "transMIN" each have an area in η-ϕ space of $\Delta\eta\Delta\phi = 4\pi/6$. When looking at multiplicities MAX and MIN refer to the number of charged particles. When we consider PTsum, then MAX and MIN refer to the scalar p_T sum of charged particles and when we consider ETsum, then MAX and MIN refer to the scalar E_T sum of particles (or calorimeter towers). The overall

"transverse" region which correspond to the average of the "transMAX" and "transMIN" densities.

As illustrated in Fig. 6, one expects that "transMAX" will pick up the hardest initial or final-state radiation while both "transMAX" and "transMIN" should receive "beam-beam remnant" contributions. Hence one expects "transMIN" to be more sensitive to the "beam-beam remnant" component of the "underlying event". This idea, was first suggested by Bryan Webber, and implemented by in a paper by Jon Pumplin [8].

Fig. 26 shows the corrected data at 1.96 TeV on the density of charged particles for the "transMAX" region , "transMIN" region, and the "transDIF" (*i.e.* transMAX – transMIN) for "leading jet" events as a function of the leading jet p_T compared with PYTHIA Tune A (with multiple parton interactions) and HERWIG (without multiple parton interactions) at the particle level (*i.e.* generator level). Similarly Fig. 27 and Fig. 28 shows the corrected data at 1.96 TeV on the PTsum and ETsum density, respectively, for the "transMAX" region , "transMIN" region, and the "transDIF" (*i.e.* transMAX – transMIN) for "leading jet" events as a function of the leading jet p_T compared with PYTHIA Tune A and HERWIG. For all three densities (number, PTsum, ETsum) PYTHIA Tune A is low, but in all three cases it agrees with the "transDIF". This indicates that the excess activity seen in the data over PYTHIA Tune A arises from the "soft" component of the "underlying event" (*i.e.* beam-beam remnants and/or multiple parton interactions) that contributes equally to both "transMAX" and "transMIN".

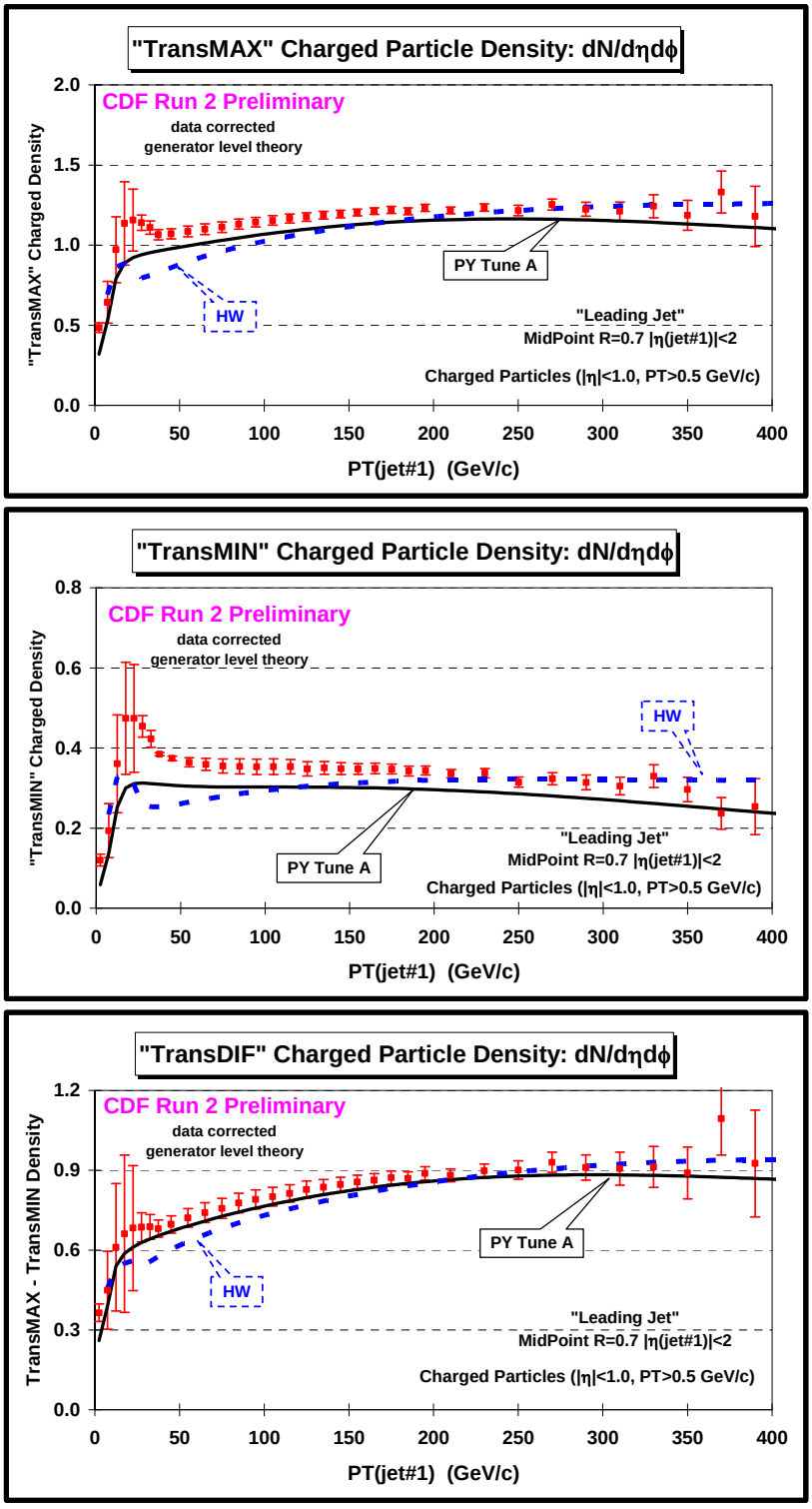

Fig. 26. Data at 1.96 TeV on the density of charged particles, $dN/d\eta d\phi$, with $p_T > 0.5$ GeV/c and $|\eta| < 1$ for the "transMAX" region (*top*), "transMIN" region (*middle*), and the "transDIF" (*i.e.* transMAX – transMIN) (*bottom*) for "leading jet" events as a function of the leading jet p_T. The data are corrected to the particle level (with errors that include both the statistical error and the systematic uncertainty) and are compared with PYTHIA Tune A (with multiple parton interactions) and HERWIG (without multiple parton interactions) at the particle level (*i.e.* generator level).

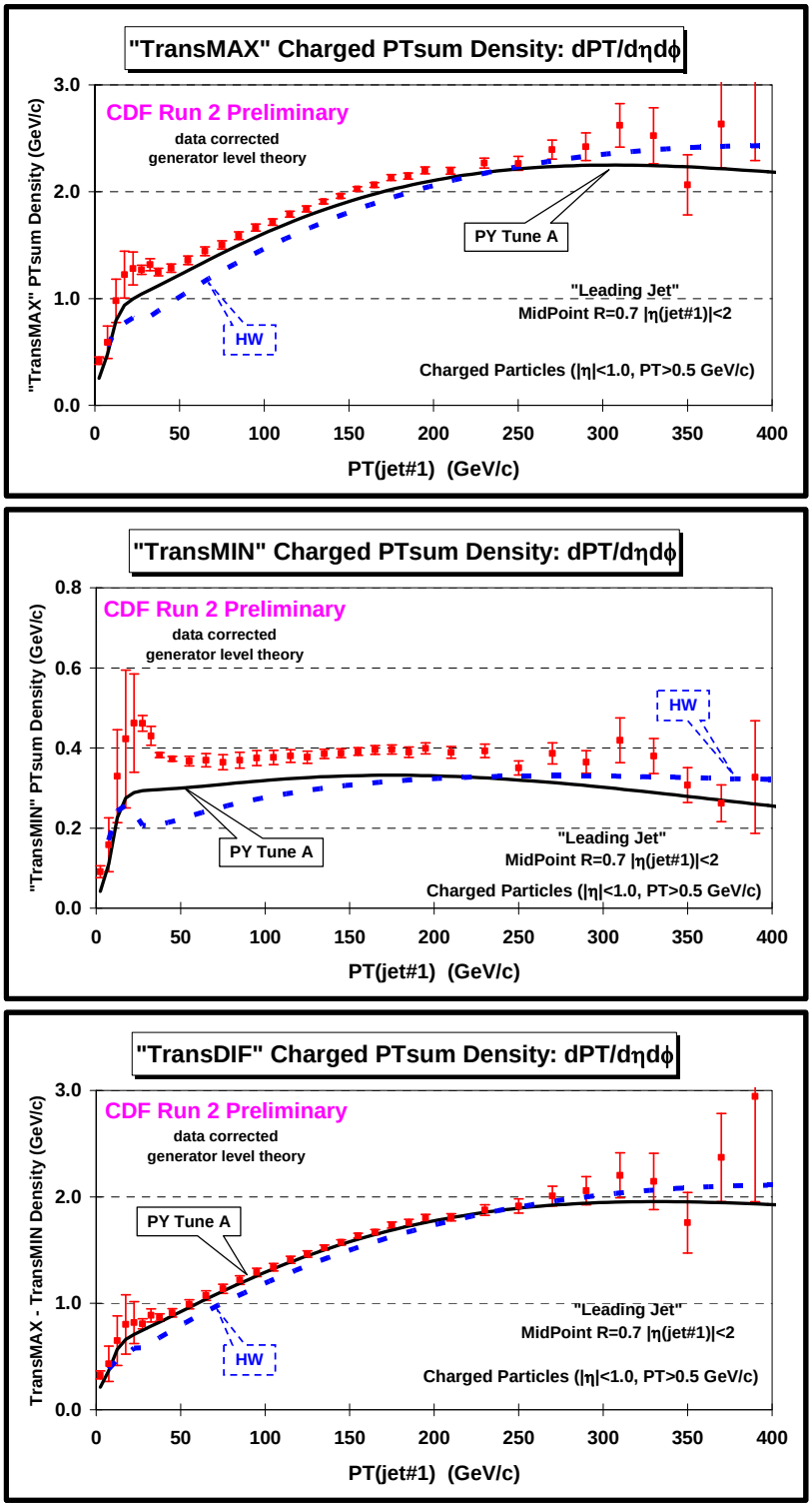

Fig. 27. Data at 1.96 TeV on the charged *scalar* p_T sum density, dPT/dηdϕ, with $p_T > 0.5$ GeV/c and $|\eta| < 1$ for the "transMAX" region (*top*), "transMIN" region (*middle*), and the "transDIF" (*i.e.* transMAX – transMIM) (*bottom*) for "leading jet" events as a function of the leading jet p_T. The data are corrected to the particle level (with errors that include both the statistical error and the systematic uncertainty) and are compared with PYTHIA Tune A (with multiple parton interactions) and HERWIG (without multiple parton interactions) at the particle level (*i.e.* generator level).

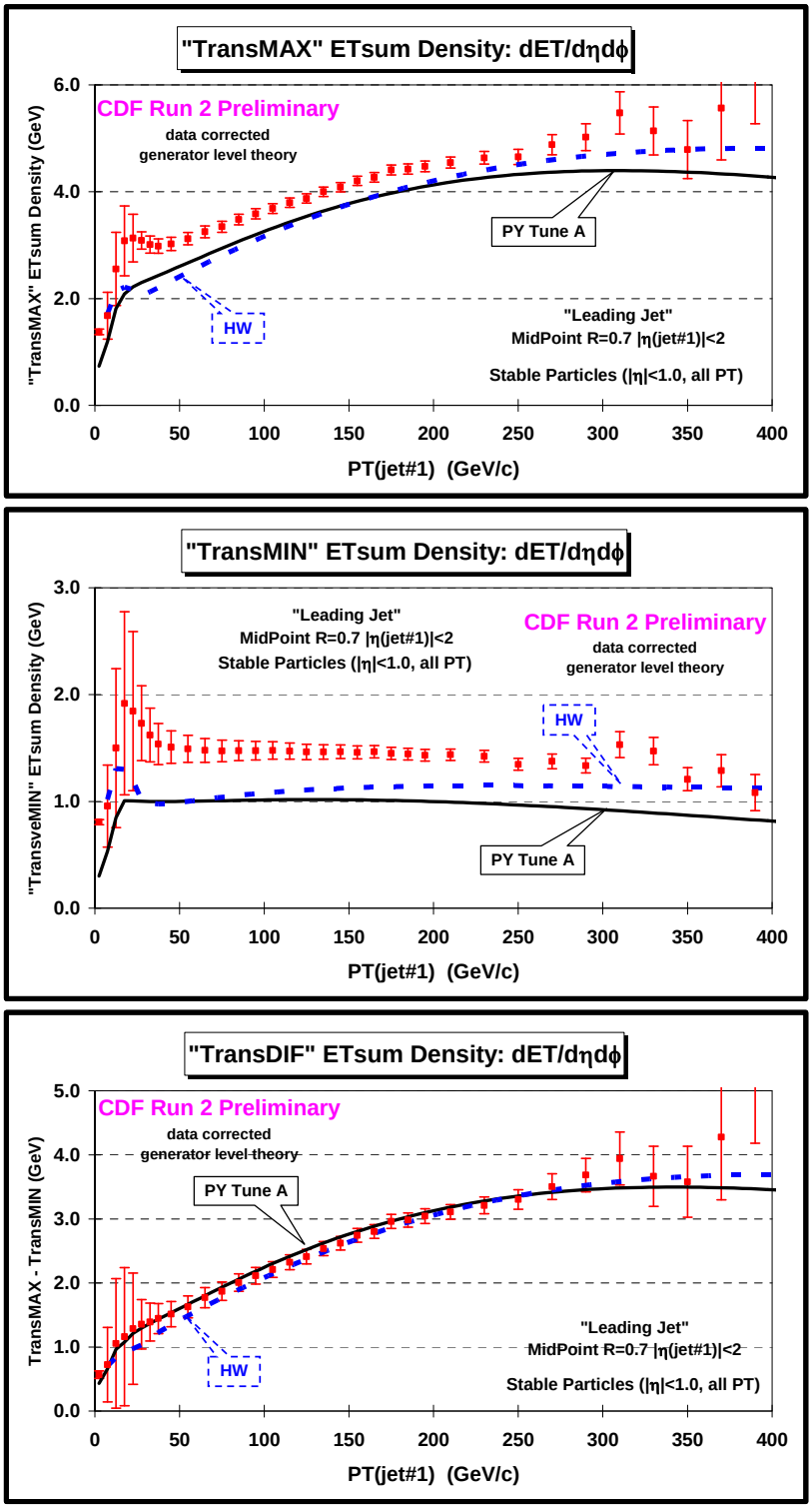

Fig. 28. Data at 1.96 TeV on the *scalar* E_T sum density, dET/dηdϕ, with $|\eta| < 1$ for the "transMAX" region (*top*), "transMIN" region (*middle*), and the "transDIF" (*i.e.* transMAX – transMIM) (*bottom*) for "leading jet" events as a function of the leading jet p_T. The data are corrected to the particle level (with errors that include both the statistical error and the systematic uncertainty) and are compared with PYTHIA Tune A (with multiple parton interactions) and HERWIG (without multiple parton interactions) at the particle level (*i.e.* generator level).

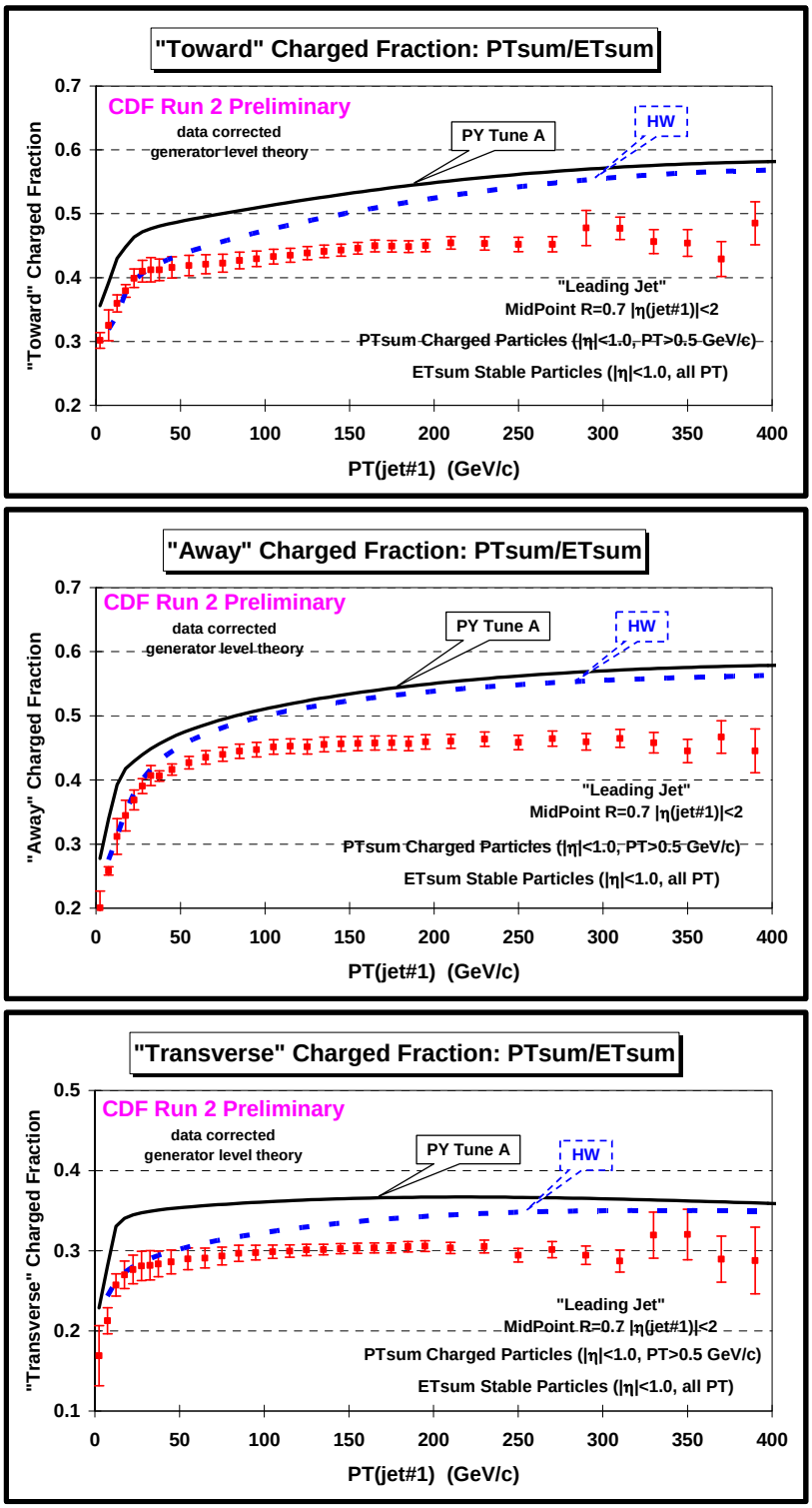

Fig. 29. Data at 1.96 TeV on the charged fraction, PTsum/ETsum, where PTsum is the *scalar* p_T sum of charged particles (p_T < 0.5 GeV/c, $|\eta| < 1$) and ETsum is the *scalar* E_T sum of all stable particles (all p_T, $|\eta| < 1$) for the "toward" region (*top*), "away" region (*middle*), and the "transverse" region (*bottom*) of "leading jet" events as a function of the leading jet p_T. The data are corrected to the particle level (with errors that include both the statistical error and the systematic uncertainty) and are compared

with PYTHIA Tune A (with multiple parton interactions) and HERWIG (without multiple parton interactions) at the particle level (*i.e.* generator level).

(8) The "Toward", "Away", and "Transverse" Charged Fraction

Both PYTHIA Tune A and HERWIG agree better with the number density and PTsum density than they do with the energy density and as can be seen in Fig. 29 both predict a charged fraction, PTsum/ETsum, that is larger that the data. Fig. 16 shows that the true "transverse" charged fraction (all p_T) is the same for PYTHIA Tune A and HERWIG and equal to about 50%. Constructing PTsum from charged particles with $p_T > 0.5$ GeV reduces the "transverse" charged fraction to about 35% for PYTHIA Tune A and slightly less for HERWIG (since it has a "softer" p_T distribution), while the "transverse" charged fraction seen in the data is about 30%. PYTHIA Tune A is off by around 17%.

V. Summary

The goal of this analysis is to produce data that can be used by the theorists to tune and improve the QCD Monte-Carlo models. The data are corrected to the particle level so that it can be used to compare to the QCD Monte-Carlo models without requiring CDF detector simulation (*i.e.* CDFSIM). We study charged particles with $p_T > 0.5$ GeV/c and $|\eta| < 1$ and calorimeter towers with $E_T > 0.1$ GeV and $|\eta| < 1$ in the "toward", "away" and "transverse" regions of h-f space relative to the leading jet. The "toward" and "away" regions are sensitive to the outgoing high p_T jets, while the "transverse" region is perpendicular to the plane of the hard 2-to-2 scattering and is therefore very sensitive to the "underlying event".

We also study four distinct jet topologies ("leading jet", "Back-to-back Inc2jet", "Back-to-back Exc2jet", and "leading chgjet"). By comparing the four jet topologies one can disentangle the various components of the "underlying event". For example, by comparing the inclusive and exclusive back-to-back 2-jet topologies one learns about the importance of contributions from third jet. It is important to provide enough plots to show the overall picture. For example, tuning the Monte-Carlo to produce more activity in the "transverse" region may destroy the agreement in the "toward" region etc.. In this note we show only the "leading jet" results. The other three topologies will be presented in subsequent notes.

Neither PYTHIA Tune A (with multiple parton interactions) or HERWIG (without multiple parton interactions) produce enough activity in the "transverse" region. PYTHIA Tune A does a much better job than HERWIG, but it is produces slightly too few charged particles and charged PTsum in both the "transMAX" and "transMIN" regions. Furthermore neither PYTHIA Tune A or HERWIG produce enough energy in the "transMAX" and "transMIN" region. However, PYTHIA Tune A does fit the charged particle, charged PTsum, and energy density for "transDIF" (*i.e.* "transMAX" minus "transMIN"). This indicates that the excess activity seen in the data over PYTHIA Tune A arises from the "soft" component of the "underlying event" (*i.e.* beam-beam remnants and/or multiple parton interactions) that contributes equally to both "transMAX" and "transMIN".

HERWIG (without multiple parton interactions) produces a "softer" distribution of charged particles in the "transverse" region and does not fit the average p_T and the PTmax in this

region, while PYTHIA Tune A (with multiple parton interactions) does a better job of fitting the data.

Acknowledgements

R. Field would like to thank Rob Roser, Jaco Konigsberg, and Mike Lindgren for arranging it so that he could work at CDF during the summer and complete this analysis.

References and Footnotes

1. T. Sjostrand, Phys. Lett. **157B**, 321 (1985); M. Bengtsson, T. Sjostrand, and M. van Zijl, Z. Phys. **C32**, 67 (1986); T. Sjostrand and M. van Zijl, Phys. Rev. **D36**, 2019 (1987).
2. *Charged Jet Evolution and the Underlying Event in Proton-Antiproton Collisions at 1.8 TeV*, The CDF Collaboration (T. Affolder et al.), Phys. Rev. **D65**, 092002, (2002).
3. *The Underlying Event in Large Transverse Momentum Charged Jet and Z-boson Production at 1.8 TeV*, talk presented by Rick Field at DPF2000, Columbus, OH, August 11, 2000.
4. *A Comparison of the Underlying Event in Jet and Min-Bias Events*, talk presented by Joey Huston at DPF2000, Columbus, OH, August 11, 2000. *The Underlying Event in Jet and Minimum Bias Events at the Tevatron*, talk presented by Valeria Tano at ISMD2001, Datong, China, September 1-7, 2001.
5. *Min-Bias and the Underlying Event at the Tevatron and the LHC*, talk presented by R. Field at the Fermilab ME/MC Tuning Workshop, Fermilab, October 4, 2002. *Toward an Understanding of Hadron Collisions: From Feynman-Field until Now*, talk presented by R. Field at the Fermilab Joint Theoretical Experimental "Wine & Cheese" Seminar, Fermilab, October 4, 2002.
6. G. Marchesini and B. R. Webber, Nucl. Phys **B310**, 461 (1988); I. G. Knowles, Nucl. Phys. B310, 571 (1988); S. Catani, G. Marchesini, and B. R. Webber, Nucl. Phys. **B349**, 635 (1991).
7. *Using MAX/MIN Transverse Regions to Study the Underlying Event in Run 2 at the Tevatron*, Alberto Cruz, Rick Field, and Craig Group, CDF/ANAL/CDF/CDFR/7703 (2005); *The Underlying Event in Run 2*, Rick Field, CDF/ANAL/CDF/CDFR/6403 (2003); *Using MAX/MIN Transverse Regions and Associated Densities to Study the Underlying Event*, A. Cruz and R. Field, CDF/ANAL/CDF/CDFR/6759, November 2003; *Jet Topologies in Min-Bias and Hard Collisions in Run 2 at the Tevatron*, A. Cruz and R. Field, CDF/ANAL/CDF/CDFR/6819, December 2003; *Using Correlations in the Transverse Region to Study the Underlying Event in Run 2 at the Tevatron*, A. Cruz and R. Field, CDF/PUB/JET/PUBLIC/6821, December 2003.
8. *Hard Underlying Event Corrections to Inclusive Jet Cross-Sections*, Jon Pumplin, Phys. Rev. **D57**, 5787 (1998).